Membrane Deformation – Finite Elements – Parametric Shape Optimization on the Koch Snowflake

Nizar Riane, Claire David, François Vigneron

Membrane Deformation – Finite Elements – Parametric Shape Optimization on the Koch Snowflake

Nizar Riane[†], Claire David[‡] [*], François Vigneron[♮]

February 11, 2025

[†] Université Mohammed V de Rabat, FSJESR-Agdal, Maroc[1]

[‡] Sorbonne Université
CNRS, UMR 7598, Laboratoire Jacques-Louis Lions, 4, place Jussieu 75005, Paris, France[2]

[♮] Université de Reims Champagne-Ardenne
CNRS, UMR 8050, Laboratoire d'Analyse et de Mathématiques Appliquées, Paris, France[3]

Abstract

We introduce the finite element method to analyze a membrane with a Koch snowflake-shaped boundary. The fractal nature of this domain presents unique challenges due to its intricate boundary structure. Our approach involves discretizing the domain, estimating the error, and proving convergence. With these aspects addressed, we solve a shape optimization problem to determine the optimal thickness of the membrane. These findings provide valuable insights into how fractal boundaries affect structural performance and optimization.

MSC Classification: 28A80 – 35J05 – 35R02.

Keywords: Fractals; Koch Snowflake; Poisson equation; membrane problem; finite elements; parametric shape optimization.

Contents

[*]The research of C. D. is supported by the MITI CNRS Conditions Extrêmes and by the ANR FRACTALS (ANR-24-CE45-3362).

[1]nizar.riane@gmail.com
[2]Claire.David@Sorbonne-Universite.fr
[3]francois.vigneron@univ-reims.fr

Acknowledgements: The authors would like to thank Michel L. Lapidus, Anna Rozanova-Pierrat and Alexander Teplyaev for their valuable comments, which have greatly contributed to enhance this work. The authors are also grateful to Kaj Nyström for providing them the counterample about H^2 regularity which is in the paper version of his thesis.

1 Introduction

In the 90's, the french physicist Bernard Sapoval and his collaborators conducted experiments devoted to the study of the vibration modes of irregular drums, especially, in the case of a fractal boundary (or, to be more precise, of a prefractal boundary, i.e., a polyhedral approximation of the given fractal). The drums consisted in a thick polyethylene film (5 mm), stretched across the prefractal boundary, which had the form of *a square Koch fractal curve* (or *Minkowski fractal*; see Benoît Mandelbrot's book [Man83], Plate 32). The drums were excited by an acoustic source (a loudspeaker) located one meter above the drum; see [Sap89], [SGM91], [SG93], [HS98] for further details. The observed and recorded modes were rather surprising: in fact, if modes were localized to four bounded regions, it was possible to excite each of these regions separately, just by moving the acoustic source, in complete contradiction with the well-known behavior of smooth domains. Those localization phenomena resulted in exceptional damping properties.

Following this work, a sharp mathematical study was done by Michel L. Lapidus and his collaborators, along with numerical simulations, devoted to the study and understanding of the eigenfunctions of the Dirichlet Laplacian on a Koch snowflake domain; see [LNRG96]. The algorithm was based on the finite difference method; in particular, the authors obtained approximations of the first fifty smallest eigenvalues, along with the associated eigenfunctions. In contrast to the aforementioned experiments, no localization phenomena were observed.

We hereafter propose to carry on the exploration of those fractal drums, by means of the finite element method, suitably implemented in the case of a domain with a fractal boundary. When the boundary has the shape of a Koch curve, it is, also, a d–set, i.e. a compact set $\mathcal{F} \subset \mathbb{R}^2$, $0 < d < 2$, such that there exists a Radon measure μ with support $\mathcal{F}$ and two strictly positive constants c_1 and c_2 satisfying, for any strictly positive number r and any ball $\mathcal{B}(X, r)$ the center of which belongs to $\mathcal{F}$,

$$c_1\, r^d \leqslant \mu\left(\mathcal{B}(X, r)\right) \leqslant c_2\, r^d\,.$$

The measure μ is then called *a d–measure*.

Formally, we can then use the Sobolev extensions theorems associated to d–sets (such as, for instance, the ones given by Peter Wilcox Jones in [Jon81]), along with Alf Jonsson and Hans Wallin's

trace theorems (see [JW84]). This enables us to properly solve the associated Poisson problem.

Insofar as our aim is to implement finite elements, this calls for approximation by polynomials, the degree of which will provide information related to the level of smoothness of the considered functions. More precisely, the polynomials involved are defined on the intersection of $\mathcal{F}$ with two–dimensional compacts. This is, of course, a kind of spline approximation. A powerful tool happens to be given by Markov's inequality, which, in its original form that goes back to 1889 (see [Mar48]) and states that, for any complex polynomial P of degree $\deg P$:

$$\|P'\|_{[-1,1]} \leqslant (\deg P)^2 \ \|P\|_{[-1,1]} .$$

Along these lines, Markov's inequality is preserved on the set $\mathcal{F}$ if, for any polynomial P with d variables, any point $X \in \mathcal{F}$ and any real number $r \in]0,1]$:

$$\max_{\mathcal{F} \cap \mathcal{B}(X,r)} |\nabla P| \leqslant \frac{c\,(P,d,\mathcal{F})}{r} \max_{\mathcal{F} \cap \mathcal{B}(X,r)} |P|$$

where $c\,(P,N,\mathcal{F})$ denotes a positive constant which depends on N, P and $\mathcal{F}$. Fortunately, as it can be found, for instance in [Wal92], d–sets preserve Markov's Inequality. Along with the fact that the aforementioned trace theorems involve Besov spaces, where functions can be approximated by splines, this makes d–sets good candidates for the finite elements method.

Indeed, as was the case if the experiments described above, we do not work with the fractal boundary itself, but, instead, with the sequence of prefractal polygonal approximations (in our case, *iterated fractal drums* (*ifs*), as introduced in [DL22]), which are Lipschitz. We are then able to prove the weak convergence of the sequence of solutions associated with the the sequence of prefractals.

Our paper is organized as follows:

i. In Section 2, we introduce the geometry of the problem, along with the functional framework.

i. In Section 3, we introduce our parametric optimization problem, in connection with the compliance properties of the involved membrane (a Koch snowflake membrane); i.e., the properties associated to the elastic deformation of the membrane, when undergoing the excitation. The considered domain is of particular interest for being both fractal and with a fractal boundary.

ii. In Section 4, we introduce the finite element method on our domain with a fractal boundary, along with the associated numerical analysis.

iii. In Section 5, we solve a shape optimization problem involving the Koch snowflake. In particular, we obtain the optimal thickness.

2 Geometric and Functional Framework

2.1 The Koch Curve and the Koch Snowflake

Henceforth, we place ourselves in the Euclidean plane, equipped with a direct orthonormal frame. The usual Cartesian coordinates are denoted by (x, y). The horizontal and vertical axes will be respectively referred to as $(x'x)$ and $(y'y)$.

Notation 1 (**Set of all Natural Numbers and Intervals**)**.** As in Bourbaki [Bou04] (Appendix E. 143), we denote by $\mathbb{N} = \{0,\, 1,\, 2,\, \ldots\}$ the set of all natural numbers and set $\mathbb{N}^\star = \mathbb{N} \setminus \{0\}$.

Given a, b with $-\infty \leqslant a \leqslant b \leqslant \infty$, $]a, b[= (a, b)$ denotes an open interval, while, for example, $]a, b] = (a, b]$ denotes a half–open, half–closed interval.

Notation 2 (**Rotation Matrix**). For $\theta \in \mathbb{R}$, we denote by $\mathcal{R}_{O,\theta}$ the following rotation matrix,

$$\mathcal{R}_{O,\theta} = \begin{pmatrix} \cos\theta & -\sin\theta \\ \sin\theta & \cos\theta \end{pmatrix} .$$

Property 2.1 (**The Koch Snowflake as a Self–Similar Set [HOP92]**). *The Koch Snowflake $\mathfrak{KS}$ is the bounded domain, the boundary of which is defined as the union of three rotated copies of Koch curves $\mathfrak{KC}$; in particular, each curve is a self–similar set with respect to the family of similarities $\{f_1, f_2, f_3, f_4\}$ defined for any $X \in \mathbb{R}^2$, by*

$$f_1(X) = \frac{1}{3}\,X + \begin{pmatrix} -\frac{1}{\sqrt{3}} \\ \frac{1}{3} \end{pmatrix} \quad ; \quad f_2(X) = \frac{1}{3}\,\mathcal{R}_{O,\frac{\pi}{3}}\,X + \begin{pmatrix} 0 \\ \frac{2}{3} \end{pmatrix} \quad ; \quad f_3(X) = \frac{1}{3}\,\mathcal{R}_{O,\frac{-\pi}{3}}\,X + \begin{pmatrix} 0 \\ \frac{2}{3} \end{pmatrix} ;$$

$$f_4(X) = \frac{1}{3}\,X + \begin{pmatrix} \frac{1}{\sqrt{3}} \\ \frac{1}{3} \end{pmatrix} ,$$

where, for $\theta \in \mathbb{R}$, the rotation matrix $\mathcal{R}_{O,\theta}$ has been introduced in Notation 2, on page 4.

The respective fixed points of the similarities $\{f_1, \ldots, f_4\}$ will be denoted by $\left\{P_1^f, \ldots, P_4^f\right\}$. Note that

$$P_1^f = \begin{pmatrix} -\frac{\sqrt{3}}{2} \\ \frac{1}{2} \end{pmatrix} \quad ; \quad P_2^f = \begin{pmatrix} -\frac{\sqrt{3}}{7} \\ \frac{5}{7} \end{pmatrix} \quad ; \quad P_3^f = \begin{pmatrix} \frac{\sqrt{3}}{7} \\ \frac{5}{7} \end{pmatrix} \quad ; \quad P_4^f = \begin{pmatrix} \frac{\sqrt{3}}{2} \\ \frac{1}{2} \end{pmatrix} .$$

The two other copies of the Koch curves are obtained by rotating the Koch curve $\mathfrak{KC}$, i.e.,

$$\partial\mathfrak{KS} = \mathfrak{KC} \cup \mathfrak{h}_1(\mathfrak{KC}) \cup \mathfrak{h}_2(\mathfrak{KC}) ,$$

where $\mathfrak{h}_1$ and $\mathfrak{h}_2$ are respectively given by

$$\forall\, X \in \mathbb{R}^2 : \quad \mathfrak{h}_1(X) = \mathcal{R}_{O,-\frac{2\pi}{3}}\,X \quad \textit{and} \quad \mathfrak{h}_2(X) = \mathcal{R}_{O,\frac{2\pi}{3}}\,X\cdot$$

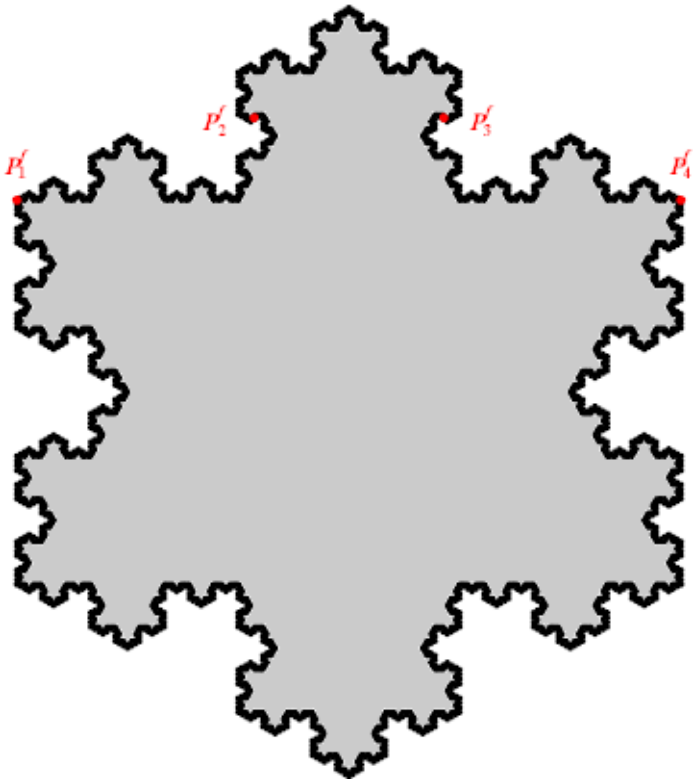

Figure 1 – Koch Snowflake.

Property 2.2 (**Self–Similarity of the Koch Snowflake**). *The Koch Snowflake is self–similar, with respect to the family of contractions* $\{g_1, \ldots, g_7\}$*, such that, for any* $X \in \mathbb{R}^2$*,*

$$g_1(X) = \frac{1}{3}\,X + \begin{pmatrix} -\dfrac{1}{\sqrt{3}} \\ -\dfrac{1}{3} \end{pmatrix} \quad ; \quad g_2(X) = \frac{1}{3}\,X + \begin{pmatrix} 0 \\ \dfrac{2}{3} \end{pmatrix} \quad ; \quad g_3(X) = \frac{1}{3}\,X + \begin{pmatrix} \dfrac{1}{\sqrt{3}} \\ -\dfrac{1}{3} \end{pmatrix} \; ;$$

$$g_4(X) = \frac{1}{\sqrt{3}}\;\mathcal{R}_{O,\frac{\pi}{6}}\,X\,;$$

$$g_5(X) = \frac{1}{3}\,X + \begin{pmatrix} -\dfrac{1}{\sqrt{3}} \\ \dfrac{1}{3} \end{pmatrix} \quad , \quad g_6(X) = \frac{1}{3}\,X + \begin{pmatrix} 0 \\ \dfrac{2}{3} \end{pmatrix} \quad ; \quad g_7(X) = \frac{1}{3}\,X + \begin{pmatrix} \dfrac{1}{\sqrt{3}} \\ \dfrac{1}{3} \end{pmatrix} .$$

The respective fixed points of the contractions $\{g_1, \ldots, g_7\}$ *will be denoted by* $\{P_1^g, \ldots, P_7^g\}$*. Note that*

$$P_1^g = \begin{pmatrix} -\dfrac{\sqrt{3}}{2} \\ -\dfrac{1}{2} \end{pmatrix} \quad ; \quad P_2^g = \begin{pmatrix} 0 \\ -1 \end{pmatrix} \quad ; \quad P_3^g = \begin{pmatrix} \dfrac{\sqrt{3}}{2} \\ -\dfrac{1}{2} \end{pmatrix} \quad ; \quad P_4^g = \begin{pmatrix} 0 \\ 0 \end{pmatrix} ;$$

$$P_5^g = \begin{pmatrix} -\dfrac{\sqrt{3}}{2} \\ \dfrac{1}{2} \end{pmatrix} \quad ; \quad P_6^g = \begin{pmatrix} 0 \\ 1 \end{pmatrix} \quad ; \quad P_7^g = \begin{pmatrix} \dfrac{\sqrt{3}}{2} \\ \dfrac{1}{2} \end{pmatrix} .$$

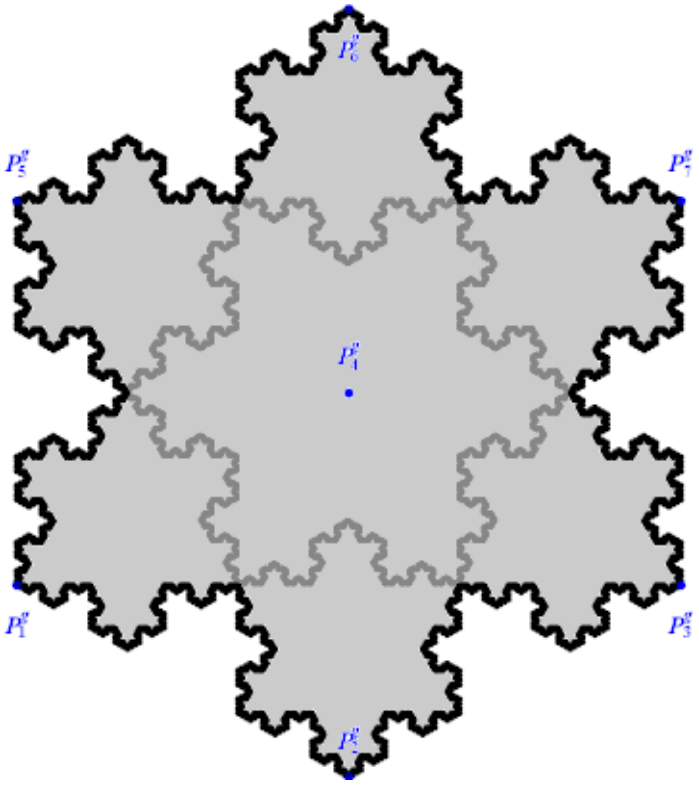

Figure 2 – The Koch Snowflake as the union of seven scaled copies of itself.

Definition 2.1 (**The Open Set Condition – Similarity Dimension**). Given $N \in \mathbb{N}^\star$, let us consider a set of similarity maps $\{f_1, \ldots, f_N\}$ and, as is done in [Hut81], the self–similar set $\mathcal{F}$ as the unique set of $\mathbb{R}^2$ such that

$$\mathcal{F} = \bigcup_{i=1} f_i(\mathcal{F}) \cdot$$

The set of maps $\{f_1, \ldots, f_N\}$ satisfies the **open set condition** if there exists a nonempty bounded open set $\mathcal{O}$ such that

$$\underset{1 \leqslant i \leqslant N}{\cup} f_i(\mathcal{O}) \subset \mathcal{O} \quad \text{and} \quad f_i(\mathcal{O}) \cap f_j(\mathcal{O}) = \emptyset \quad \text{if } i \neq j \cdot$$

In the case when the similarity maps $\{f_1, \ldots, f_N\}$ are contractions, with respective ratios $\{r_1, \ldots, r_N\} \in]0,1[^N$, there exists a real number $D_H(\mathcal{F})$ such that

$$\sum_{i=1}^{N} r_i^{D_H(\mathcal{F})} = 1\,, \tag{1}$$

called the **similarity dimension** of $\mathcal{F}$ (see [Fal03]); it is also the Hausdorff dimension of $\mathcal{F}$.

Proposition 2.3 (**Hausdorff and Similarity Dimension of the Koch Snowflake**). *The respective Hausdorff dimensions of the Koch Snowflake* $\mathfrak{KS}$ *and of its boundary* $\partial\mathfrak{KS} = \mathfrak{KC} \cup \mathfrak{h}_1(\mathfrak{KC}) \cup \mathfrak{h}_2(\mathfrak{KC})$ *(see Property 2.1, on page 4), are given by*

$$D_H(\mathfrak{KS}) = 2 \quad \textit{and} \quad D_H(\partial\mathfrak{KS}) = \frac{\ln(4)}{\ln(3)} \cdot$$

Note that they coincide with the similarity dimension; see [Fal03].

Proof. This directly follows from the definition of the similarity dimension (see Definition 2.1, on page 6 just above) since

$$\sum_{i=1}^{4}\left(\frac{1}{3}\right)^{D_H(\mathfrak{KC})}=1 \quad \text{and} \quad \left(\frac{1}{\sqrt{3}}\right)^{D_H(\mathfrak{KS})}+\sum_{i=1}^{6}\left(\frac{1}{3}\right)^{D_H(\mathfrak{KS})}=1\cdot$$

□

Definition 2.2 (**Initial Points – Initial Segment**)**.** We define the *initial points*, respectively denoted by I and J as being the fixed points respectively associated with the similarities f_1 and f_4 introduced in Property 2.1, on page 4; in fact, we have that

$$I=P_1^f=\begin{pmatrix}-\frac{\sqrt{3}}{2}\\ \frac{1}{2}\end{pmatrix} \quad ; \quad J=P_4^f=\begin{pmatrix}\frac{\sqrt{3}}{2}\\ \frac{1}{2}\end{pmatrix}.$$

The line segment $[IJ]$ is called *the initial segment.*

Property 2.4 (**The Koch Curve, Limit of a Sequence of Prefractal Graphs**)**.** *The Koch Curve* $\mathfrak{KC}$ *is the limit of* the prefractal sequence *of finite graphs* $(\mathfrak{KC}_m)_{m\in\mathbb{N}}$ *such that*

$$\mathfrak{KC}_0=[IJ] \quad \textit{and } \forall\, m\in\mathbb{N}^\star: \quad \mathfrak{KC}_m=\bigcup_{\mathcal{W}\in\Sigma_m} f_{\mathcal{W}}(\mathfrak{KC}_0)\,,$$

where the points I and J have been introduced in Definition 2.2, on page 7 just above and where, for any $m\in\mathbb{N}^\star$, $\Sigma_m=\{1,2,3,4\}^m$, with $f_{\mathcal{W}}$ denoting a composition of maps from $\{f_1,\ldots,f_4\}$ and indexed by $\mathcal{W}$; see Figure 3, on page 7.

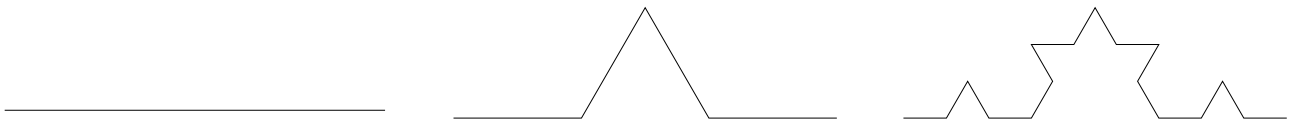

Figure 3 – The prefractals curves $\mathfrak{KC}_0$, $\mathfrak{KC}_1$ and $\mathfrak{KC}_2$.

Property 2.5 (**The Koch Snowflake, Limit of a Sequence of Prefractal Polygonal Domains**)**.** *The Koch Snowflake* $\mathfrak{KS}$ *is the limit of* the prefractal sequence *of polygonal domains* $(\mathfrak{KS}_m)_{m\in\mathbb{N}}$ *where, for any $m\in\mathbb{N}^\star$, $\mathfrak{KS}_{\mathfrak{m}}$ is* the m^{th}–prefractal Snowflake*, which is the bounded domain of $\mathbb{R}^2$ delimited by the three copies $\{\mathfrak{KC}_m;\mathfrak{h}_1(\mathfrak{KC}_m);\mathfrak{h}_2(\mathfrak{KC}_m)\}$; see Figure 4, on page 8. Note that, for any $m\in\mathbb{N}^\star$,*

$$\partial\mathfrak{KS}_m=\mathfrak{KC}_m\cup\mathfrak{h}_1(\mathfrak{KC}_m)\cup\mathfrak{h}_2(\mathfrak{KC}_m)\,.$$

Definition 2.3 (**Sets of Vertices, Prefractals**)**.** We introduce *the initial boundary set* $\mathcal{I}_0=\{I,J\}$, where the points I and J have been given in Definition 2.2, on page 7 above.

We then set for any $m\in\mathbb{N}^\star$,

$$V_m^{\mathcal{I}}=\bigcup_{i=1}^{N} f_i\left(V_{m-1}^{\mathcal{I}}\right)=\bigcup_{\mathcal{W}\in\Sigma_m} f_{\mathcal{W}}\left(\mathcal{I}_0\right)\ \cdot$$

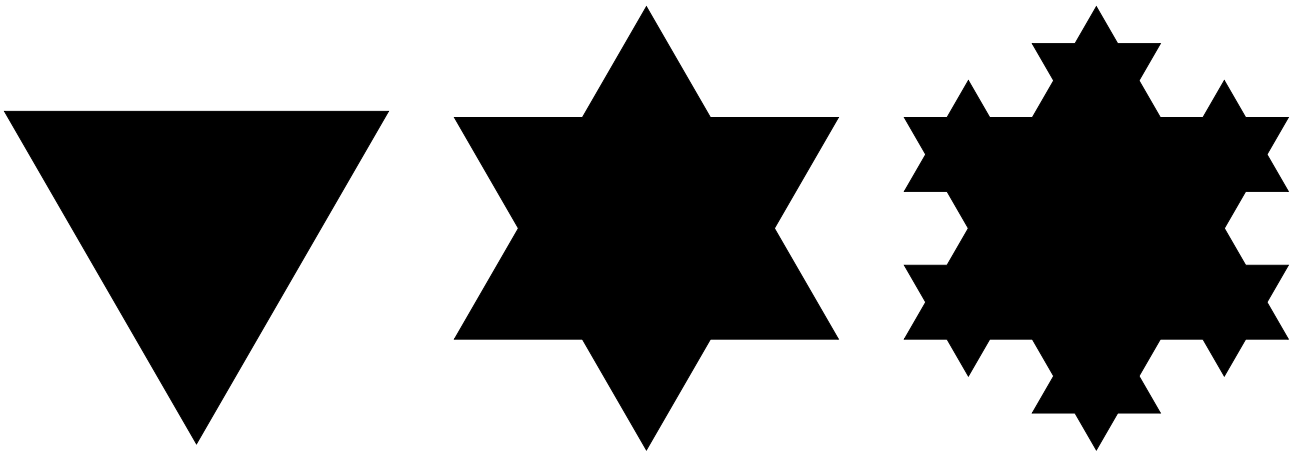

Figure 4 – The polygonal domains $\mathfrak{KS}_0$, $\mathfrak{KS}_1$ and $\mathfrak{KS}_2$.

For any $m \in \mathbb{N}$, the set of points $V_m^{\mathcal{I}}$, where two consecutive points are connected, is an undirected finite graph, called the $\boldsymbol{m^{th}}$**–prefractal graph** and denoted by $\mathfrak{KC}_m$. Observe that, for any $m \in \mathbb{N}$, the set of points of $V_m^{\mathcal{I}}$ also corresponds to the set of vertices of $\mathfrak{KC}_m$. Therefore, $V_m^{\mathcal{I}}$ is naturally called *the set of vertices* of the prefractal $\mathfrak{KC}_m$.

We set $V^{\mathcal{I},\star} = \bigcup_{m \geqslant 0} V_m^{\mathcal{I}}$ and recall that $\mathfrak{KC} = \overline{V^{\mathcal{I},\star}}$ (see [Hut81]).

Definition 2.4 (**Adjacent Vertices, Edge Relation**)**.** For any $m \in \mathbb{N}$, two vertices X and Y belonging to $V_m^{\mathcal{I}}$ will be said to be *adjacent* (i.e., *neighboring* or *junction points*) if and only if the edge XY belongs to $\partial\mathfrak{KS}_m$; we then write $X \underset{m}{\sim} Y$. Note that this edge relation depends on m, which means that points adjacent in $V_m^{\mathcal{I}}$ might not remain adjacent in $V_{m+1}^{\mathcal{I}}$.

2.2 Sobolev Spaces – Traces – Weak Formulation

Notation 3 (**Lebesgue Measure on** $\mathbb{R}^2$)**.** We hereafter denote by $\mu_{\mathcal{L}}$ the Lebesgue measure on $\mathbb{R}^2$.

Notation 4 (**Boundary Measure on the Boundary of the Snowflake**)**.** In the sequel, we denote by $\mu_{\partial\mathfrak{KS}}$ the boundary measure on the boundary $\partial\mathfrak{KS}$ of the Snowflake.

Remark 2.1. In practice, $\mu_{\partial\mathfrak{KS}}$ is a $D_H\left(\partial\mathfrak{KS}\right)$–measure; see Definition 2.7, on page 9, along with Proposition 2.6, on page 10 below.

2.2.1 (ϵ, δ)–Domains, John Domains and d–sets

Notation 5 (**Euclidean Distance**)**.** In the sequel, we denote by d_{eucl} the Euclidean distance on $\mathbb{R}^2$.

Definition 2.5 ((ϵ, δ)–**Domains [Jon81]**)**.** Given $\epsilon > 0$ and $0 < \delta \leqslant \infty$, an open connected subset $\Omega \subset \mathbb{R}^n$ is called an (ϵ, δ)-*domain* if, for every pair of points $(X, Y) \in \Omega^n 2$ such that $d_{eucl}(X, Y) < \delta$, there exists a rectifiable arc $\gamma \subset \Omega$, with length $\ell(\gamma)$ joining X to Y and satisfying

i. $\ell(\gamma) \leqslant \dfrac{d_{eucl}(X, Y)}{\epsilon}$.

ii. $\forall\, Z \in \gamma : \quad d_{eucl}(Z, \partial\Omega) \geqslant \dfrac{\epsilon\, d_{eucl}(X, Z)\, d_{eucl}(Y, Z)}{d_{eucl}(X, Y)}$.

Definition 2.6 (**John Domains [Joh61]**). An open connected subset $\Omega \subset \mathbb{R}^n$ is called a **John domain** if there exist two real numbers $\alpha > 0$ and $\beta > 0$, along with a point $X \in \Omega$ called the **center of** Ω such that for every point $Y \in \Omega$ we can find a rectifiable arc $\gamma \subset \Omega$, with length $\ell(\gamma) \leqslant \beta$ joining X to Y and satisfying

$$\forall\, Z \in \gamma : \quad d_{eucl}(Z, \partial\Omega) \geqslant \alpha\, \ell(\gamma(Z, Y))\,.$$

Remark 2.2 (**Connection between John Domains and** (ϵ, δ)**–domains – Some Examples [JW84]**).
i. (ϵ, δ)–domains are John domains; see Figure 5, on page 9, for the (ϵ, δ) and John conditions.
ii. The Koch Snowflake $\mathfrak{KS}$ is an(ϵ, δ)–domain and therefore also a John domain.

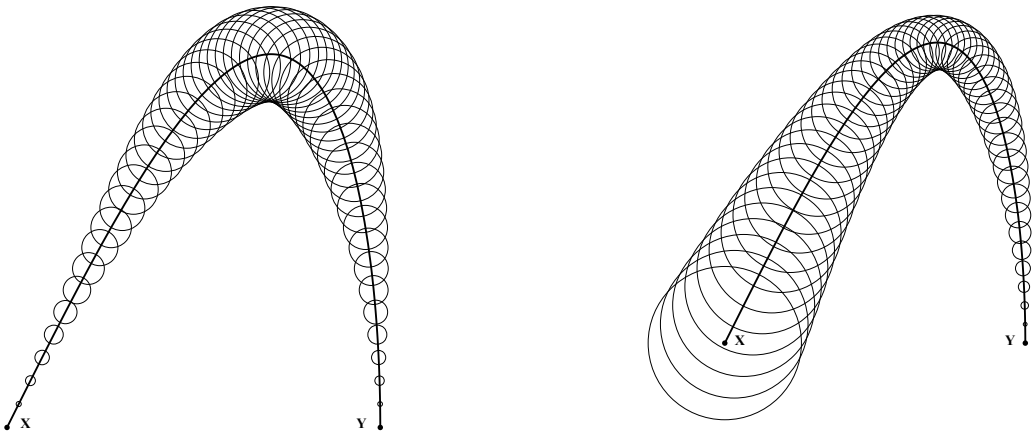

(ϵ, δ) condition. John condition.

Figure 5 – An (ϵ, δ) domain and a John domain.

Notation 6 (**Wave Inequality Symbol**). Given two positive numbers a and b, we will use the notation $a \lesssim b$ when there exists a strictly positive constant C such that $a \leqslant C\, b$.

Definition 2.7 (***d*–Measure – *d*–set ([JW84], page 28)**). Let us denote by F a closed, nonempty subset of $\mathbb{R}^n$ and d a real number such that $0 < d \leqslant n$. A positive Borel measure μ with support F is called a d–**measure on** F if, for any closed ball $\mathcal{B}(X, r)$, with center $X \in F$ and radius $r > 0$, we have that

$$r^d \lesssim \mu\left(\mathcal{B}(X, r)\right) \lesssim r^d\,.$$

A closed, nonempty subset F of $\mathbb{R}^n$ is a d–**set** $(0 < d \leqslant n)$ if there exists a d–measure on F.

Remark 2.3 (**About *d*–measures**). Examples of d–measures and d–sets can be found in the book [JW84], Chapter 2.

An important comment is that, when $0 < d \leqslant n$, suitably normalized d–measures coincides with the n–dimensional Lebesgue measure (see [Wal91], Notation page 118). This enables us, in particular, to obtain equivalent and useful characterizations of the function spaces involved, especially, the Besov spaces, as in Theorem 2.11, on page 10 below.

Proposition 2.6 (**The Boundary of the Koch Snowflake as a d–set ([Wal91], Proposition 2)**). *The boundary $\partial\mathfrak{KS}$ of the Koch Snowflake is a $\dfrac{\ln 4}{\ln 3}$–set. Note that $\dfrac{\ln 4}{\ln 3}$ is the Hausdorff dimension of the Koch Curve $\mathfrak{KC}$ mentioned in Proposition 2.3, on page 6.*

2.2.2 Function Spaces – Trace Theorems

Definition 2.8 (**Hölder Spaces [Eva10]**). Let us denote by Ω an open subset of $\mathbb{R}^n$, $\alpha > 0$ and k an integer such that $k < \alpha \leqslant k+1$. The Hölder space $C^{k,\alpha-k}(\Omega)$ is the space of $C^k(\Omega)$ functions f such that

$$\|f\|_{C^{k,\alpha-k}(\overline{\Omega})} = \sum_{|j|\leqslant k} \left\|D^j f\right\|_{C(\overline{\Omega})} + \sum_{|j|=k} \sup_{h\,\in\,\Omega} \frac{|D^j f(X+h) - D^j f(X)|}{|h|^{\alpha-k}} < \infty\,.$$

Definition 2.9 (**Sobolev Space on an Open Set $\Omega \subset \mathbb{R}^2$**). Given $k \in \mathbb{N}$ and $p \geqslant 1$, we recall that the Sobolev space on an open set $\Omega \subset \mathbb{R}^2$, denoted by $W_k^p(\Omega)$, is given by

$$W_p^k(\Omega) = \{f \in L^p(\Omega)\ ,\ \forall\,\alpha \leqslant k\,,\, D^\alpha f \in L^p(\Omega)\}\ ,$$

where $L^p(\Omega)$ denotes the Lebesgue space of order p on Ω, while, for the multiindex $\alpha \leqslant k$, $D^\alpha f$ is the classical partial derivative of order α, interpreted in the weak sense.

We denote $H^k(\Omega) = W_2^k(\Omega)$ and by $H_0^k(\Omega)$ the closure of the space test functions $\mathcal{D}(\Omega)$ in $H^k(\Omega)$. For a function $f \in H^k(\Omega)$, we denote by

$$|f|_{H_0^k(\Omega)} = \left(\sum_{|\alpha|=k} ||D^\alpha f||^2_{L^2(\Omega)}\right)^{\frac{1}{2}}$$

$$\|f\|_{H_0^k(\Omega)} = \left(\sum_{|\alpha|\leqslant k} ||D^\alpha f||^2_{L^2(\Omega)}\right)^{\frac{1}{2}}$$

Definition 2.10 (**Besov Spaces [JW84]**). Given an open subset Ω of $\mathbb{R}^n$, $\alpha > 0$, $1 \leqslant p, q \leqslant \infty$, along with an integer k such that $0 \leqslant k < \alpha \leqslant k+1$, the Besov space, or (Hölder spaces in L^p–norm) $B_\alpha^{p,q}(\Omega)$ is given by

$$B_\alpha^{p,q}(\Omega) = \left\{ f \in L^p(\Omega),\ \sum_{|j|\leqslant k} \left\|D^j f\right\|_{L^p(\Omega)} + \sum_{|j|=k} \left\{ \int_{\mathbb{R}^n} \frac{\|\Delta_h f\|^q_{L^p(\Omega)}}{|h|^{n+(\alpha-k)\,q}}\, dh \right\}^{\frac{1}{q}} < \infty \right\}\ ,$$

where Δ_h denotes the usual first difference, defined here by

$$\forall\, t \in \Omega, \forall\, h \in \mathbb{R}^n\ ,\quad \Delta_h f(t) = f(t+h) - f(t)\,.$$

Proposition 2.7 (**[JW84]**). *The space $B_\alpha^{p,q}(\Omega)$ is a Banach space for the norm $\|\cdot\|_{B_\alpha^{p,q}}$. If $1 \leqslant p, q < \infty$, then $\mathcal{D}(\Omega)$, the space of infinitely differentiable functions with compact support on Ω, is dense in $B_\alpha^{p,q}(\Omega)$.*

Definition 2.11 (**Besov Spaces on d–sets [JW84]**). Let $0 < \alpha < 1$, $1 \leqslant p \leqslant \infty$ and F a d–set with respect to a d–measure μ. A function f belongs to the Besov space $B_\alpha^{p,p}(F)$ if and only if it has finite norm

$$\|f\|_{B^{p,p}_{\alpha}} = \|f\|_{L^p_\mu} + \left(\iint_{d_{eucl}(X,Y)<1} \frac{|f(X)-f(Y)|^p}{(d_{eucl}(X,Y))^{d+\alpha\, p}}\, d\mu(X)\, d\mu(Y) \right)^{\frac{1}{p}} .$$

Theorem 2.8 (**Rellich Embedding Theorem for John Domains [CRW13]**). *If $1 \leqslant p < \infty$ and if $\Omega \subset \mathbb{R}^n$ is a John domain, the injection*

$$W^1_p(\Omega) \to L^p(\Omega)\,,$$

is a compact injection.

As a consequence, we have the following Poincaré inequality (for a more general result, we refer to [CDMP19]):

Theorem 2.9 (**Poincaré Inequality for John Domains**). *Let us denote by $\Omega \subset \mathbb{R}^n$ a John domain. Then, there exists $C > 0$ such that*

$$\forall\, f \,\in\, H^1_0(\Omega)\ , \quad \|f\|_{L^2(\Omega)} \leqslant C\, \|\nabla f\|_{L^2(\Omega)}\ .$$

The constant C is called the Poincaré constant.

Now, we introduce a trace theorem for d–sets. Let us recall that the trace operator of a function f on a set F is the operator

$$\mathbf{R}\ :\ f \to f_{|F}$$

and that an extension operator of a function g, defined on$F$, to $\mathbb{R}^n$, yields

$$\mathbf{E}\ :\ g \to \mathbf{E}g \qquad \text{such that} \qquad (\mathbf{E}g)_{|F} = g\,.$$

Theorem 2.10 (**Trace of Sobolev Spaces on d–sets [JW84]**). *Let us denote by F a d–set with respect to ta d–measure μ, α an integer, along with real numbers $0 < d < n$, $0 < \beta = \alpha - \dfrac{n-d}{p}$ and $1 < p < \infty$. The restriction operator satisfies $W^{\alpha}_p(\mathbb{R}^n)_{|F} = B^{p,p}_{\beta}(F)$, as a linear bounded operator.*

Theorem 2.11 (**Jones Extension Theorem of Sobolev Spaces [Jon81]**). *If $\Omega \subset \mathbb{R}^n$ is an (ϵ, δ)–domain, there exists a linear bounded extension operator*

$$W^{\alpha}_p(\Omega) \to W^{\alpha}_p(\mathbb{R}^n) \quad \textit{for } 1 \leqslant p \leqslant \infty \textit{ and } \alpha \geqslant 0\,.$$

Notation 7 (**Set of Real Polynomials with N Variables**). Given $n \in \mathbb{N}^\star$, we denote by $\mathbb{R}[X_1, \ldots, X_n]$ the set of real polynomials with n variables.

For the sake of concision, we will often write, with a slight abuse, $\mathbb{R}[X]$, instead of $\mathbb{R}[X_1, \ldots, X_n]$.

Definition 2.12 (**Markov Inequality**)**.** We say that a closed, nonempty subset F of $\mathbb{R}^n$ *preserves Markov's Inequality* if, for any polynom $P \in \mathbb{R}[X_1, \ldots, X_n]$, any point $X \in F$ and any real number $r \in]0, 1]$:

$$\max_{F \cap \mathcal{B}(X,r)} |\nabla P| \leqslant \frac{c\,(P, n, F)}{r} \max_{F \cap \mathcal{B}(X,r)} |P|\,,$$

where $c\,(P, n, F)$ denotes a positive constant which depends on n, P and F.

Corollary 2.12 (**Trace Operator [Wal91]**)**.** *Let $\Omega \subset \mathbb{R}^n$ be an (ϵ, δ)-domain, $\partial\Omega$ a d–set with respect to a d–measure μ, α an integer, $0 < d < n$, $0 < \beta = \alpha - \dfrac{n-d}{p}$ and $1 < p < \infty$. If $\partial\Omega$ preserves Markov's inequality; i.e., if $d > n - 1$, we then have that*

$$W_p^{\alpha}(\Omega)_{|\partial\Omega} = B_{\beta}^{p,p}(\partial\Omega)\,,$$

along with the fact that the trace operator is a linear bounded surjection; (see [Wal91], Proposition 4, page 120).

Remark 2.4 (**On the Use of the Trace Operator**). In our present setting, where the boundary is fractal, we cannot *a priori* define normal derivatives. However, since we have a trace operator, which maps Sobolev spaces on the interior of the considered domain, onto Besov spaces endowed with a scalar product (by means of the d–measure involved), we can work on the dual spaces; hence, it is possible to apprehend the normal derivative of a function belonging to the aforementioned Sobolev spaces, as en element of the Besov trace spaces.

Theorem 2.13. *If $\Omega \subset \mathbb{R}^n$ is an (ϵ, δ)–domain and if $k > \dfrac{n}{p}$, then, the Sobolev space $W_p^k(\Omega)$ is a subset of $C^0(\overline{\Omega})$, and the injection is continuous.*

Proof. According to Theorem 2.11, on page 11, there exists a linear bounded extension operator $\mathbf{E} : W_p^k(\Omega) \to W_p^k(\mathbb{R}^n)$ such that

$$(\mathbf{E}g)_{|\Omega} = g \quad \text{and} \quad \|\mathbf{E}g\|_{W_p^k(\mathbb{R}^n)} \lesssim \|g\|_{W_p^k(\Omega)}\,.$$

We can then use the following classical result to conclude:

Lemma 2.14 (**Compact Injection from W_p^k in $C^0(\mathbb{R}^n)$** [Bre99])**.** *For $k > \dfrac{n}{p}$, the injection $\iota : W_p^k(\mathbb{R}^n) \to C^0(\mathbb{R}^n)$ is compact.*

□

Theorem 2.15 (**Density**)**.** *Let us denote by $\mathring{\mathfrak{KS}}$ the interior of the Koch Snowflake $\mathfrak{KS}$. For every $u \in H^1(\mathring{\mathfrak{KS}})$, there exists a sequence of functions $(u_k)_{k\in\mathbb{N}} \subset C^{\infty}(\mathfrak{KS})$ such that*

$$\lim_{k\to\infty} \|u - u_k\|_{H^1(\mathring{\mathfrak{KS}})} = 0\,.$$

Proof. From the Jones extension theorem, there exists an extension $\bar{u} \in H^1(\mathbb{R}^2)$ such that $\bar{u}_{|\mathring{\mathfrak{KS}}} = u$ and $\|\bar{u}\|_{H^1(\mathbb{R}^2)} \leqslant \|u\|_{H^1(\mathring{\mathfrak{KS}})}$. So we can choose a function $\rho \in C^\infty(\mathbb{R}^2)$ such that

$$\forall\, x \in \mathbb{R}^2 \;:\quad \rho(x) \geqslant 0 \quad ; \quad \forall\, x \in \mathbb{R}^2, \text{ for } \|x\| \geqslant 1 \;:\quad \rho(x) = 0 \quad ; \quad \int_{\mathbb{R}^2} \rho\, dx = 1$$

and then introduce *the mollifier* $\rho_k = k^2\, \rho(kx)$. We thus have that the sequence of terms $(u_k)_{k\in\mathbb{N}} = (\bar{u} \star \rho_k)_{k\in\,\mathbb{N}}$ satisfies the theorem. □

Theorem 2.16 (**Normal Derivatives on a Fractal Boundary [Lan02]**). *If $u \in H^1(\mathring{\mathfrak{KS}})$ and $\Delta u \in L^2(\mathring{\mathfrak{KS}})$, then the normal derivative of u on the boundary exists as an element of the dual space of the trace space $H^1_{|\partial\mathfrak{KS}}(\mathring{\mathfrak{KS}})$; i.e., as an element of the dual space of $B^{2,2}_{\frac{D_H(\partial\mathfrak{KS})}{2}}(\partial\mathfrak{KS})$ (where $D_H(\partial\mathfrak{KS}) = \dfrac{\ln(4)}{\ln(3)}$); i.e., as a linear and continuous functional on $H^1_{|\partial\mathfrak{KS}}(\mathring{\mathfrak{KS}})$. More precisely, the normal derivative of u is given by*

$$\forall\, v \in H^1(\mathring{\mathfrak{KS}}) \;:\quad \big\langle \partial_n u,\, v_{|\partial\mathfrak{KS}} \big\rangle = \int_{\mathfrak{KS}} \Delta u\, v\, dx + \int_{\mathfrak{KS}} \nabla u\, \nabla v\, dx\,.$$

3 The Membrane Problem on the Koch Snowflake

The membrane problem consists in finding the solution of the following non-autonomous Poisson equation, given by

$$(\mathcal{P}_\mathcal{H}) \quad \left\{ \begin{array}{rcl} -\mathrm{div}\,(h\nabla u) & = f & \text{in } \mathring{\mathfrak{KS}}\,, \\ u & = 0 & \text{in } \partial\mathfrak{KS}\,, \end{array} \right. \tag{2}$$

By multipling the first equation of $(\mathcal{P}_\mathcal{H})$ by $v \in \mathcal{D}(\mathring{\mathfrak{KS}})$ and by applying the integration by parts formula, we get the variational Dirichlet problem

$$\forall\, v \in \mathcal{D}(\mathring{\mathfrak{KS}}) \;:\quad \int_{\mathfrak{KS}} h\, \nabla u \nabla v\, dx = \int_{\mathfrak{KS}} f\, v\, dx\,, \quad (\mathcal{D}ir) \tag{3}$$

Theorem 3.1 (**Solution of The Membrane Problem on the Koch Snowflake**). *Given $h \in L^\infty(\mathring{\mathfrak{KS}})$ such that $h_{\min} \leqslant h \leqslant h_{\max}$ and $f \in L^2(\mathring{\mathfrak{KS}})$, the following variational Dirichlet problem,*

$$\forall\, v \in \mathcal{D}(\mathring{\mathfrak{KS}}) \;:\quad \int_{\mathfrak{KS}} h\, \nabla u \nabla v\, dx = \int_{\mathfrak{KS}} f\, v\, dx\,, \quad (\mathcal{D}ir) \tag{4}$$

admits a weak solution in $H^1_0(\mathring{\mathfrak{KS}})$.

Proof. The bilinear form $(u,v) \mapsto a(u,v) = \displaystyle\int_{\mathfrak{KS}} h\, \nabla u \nabla v\, dx$ is symmetric and continuous, because

$$\forall\,(u,v) \in H^1(\mathring{\mathfrak{KS}}) \times H^1(\mathring{\mathfrak{KS}}) \;:\quad \left| \int_{\mathfrak{KS}} h\, \nabla u \nabla v\, dx \right| \leqslant h_{\max}\, \|\nabla u\|_{L^2(\mathring{\mathfrak{KS}})}\, \|\nabla v\|_{L^2(\mathring{\mathfrak{KS}})}\,.$$

It is also coercive, since

$$\forall\, u \in H^1(\mathring{\mathfrak{KS}}) \;:\quad a(u,u) = \int_{\mathfrak{KS}} h\, |\nabla u|^2\, dx \geqslant h_{\min}\, \|\nabla u\|^2_{L^2(\mathring{\mathfrak{KS}})} \geqslant \frac{h_{\min}}{C+1}\, \|u\|^2_{H^1(\mathring{\mathfrak{KS}})}\,, \tag{5}$$

where C is the Poincaré constant, introduced in Theorem 2.9, on page 11.

The map $L : v \mapsto \displaystyle\int_{\mathfrak{KS}} f\, v\, dx$ is linear and continuous. So, thanks to the Lax–Milgram theorem, we deduce that the problem $(\mathcal{D}ir)$ in relation (4) just above admits a unique solution in the Hilbert space $H_0^1(\mathring{\mathfrak{KS}})$.

□

An important question concerns the regularity of the solution u given the regularity of f. A significant and challenging result, established Kaj Nyström in [Nys94] and [Nys96], and discussed by Alf Jonsson and Hans Wallin in [JW97], shows that u does not generally belong to $H^2(\mathring{\mathfrak{KS}})$. However, we still have the interior regularity :

Theorem 3.2 (**On the Regularity of Solutions** ([Eva10] theorem 2 on page 332))**.** *Assume $h \in C^{m+1}(\mathfrak{KS})$ and $f \in H^m(\mathring{\mathfrak{KS}})$ for $m \in \mathbb{N}^\star$. Suppose $u \in H^1(\mathring{\mathfrak{KS}})$ is the weak solution of the elliptic problem*

$$-div(h\nabla u) = f \quad in\ \mathring{\mathfrak{KS}}\,.$$

Then

$$u \in H^{m+2}_{loc}(\mathring{\mathfrak{KS}})$$

and for each open set $U \subset \mathring{\mathfrak{KS}}$ we have the estimate

$$\|u\|_{H^{m+2}(\mathring{\mathfrak{KS}})} \leqslant C\left(\|f\|_{H^m(\mathring{\mathfrak{KS}})} + \|u\|_{L^2(\mathring{\mathfrak{KS}})}\right)$$

the constant C depending only on m, $\mathring{\mathfrak{KS}}$, U and h.

4 The Finite Element Method for the Koch Snowflake

4.1 Position of the Problem

Let us again consider the Dirichlet membrane problem in the variational form:

$$\int_{\mathfrak{KS}} h\,\nabla u\,\nabla v\, dx = \int_{\mathfrak{KS}} f\, v\, dx\,. \quad (\mathcal{D}ir_{var}) \tag{6}$$

For the benefit of the reader who may not be familiar with mathematical notions devoted to Lagrange finite elements, we shall first recall several definitions (see [All12] for further details).

Definition 4.1 (**Lagrange Finite Element**)**.** A **Lagrange finite element** is a triplet (K, Σ, P) such that:

i. K is a compact, convex and nonempty interior.

ii. $\Sigma = \{a_1, \ldots, a_N\}$, with $N \in \mathbb{N}^\star$, is a finite set of (distinct) points of K.

iii. P is a function vector space of finite dimension defined on K, such that Σ is unisolvent in the sense of Definition 4.2, on page 15.

Definition 4.2 (**Local Basis Functions**)**.** Let us denote by (K, Σ, P) a Lagrange finite element. We call **local basis functions** the following N functions of P, denoted by e_i, for $i = 1, \ldots, N$, such that

$$e_i(a_j) = \delta_{ij} \qquad 1 \leqslant i, j \leqslant N$$

The N–uplet $(e_1, \ldots, e_N)$ is, by construction, a basis of the vector space P.

The P–**interpolation operator** on Σ is the operator π_K that to every function g on K, associates $\pi_K\, g$ defined by

$$\pi_K\, g = \sum_{i=1}^{N} g(a_i) e_i\,.$$

This function $(\pi_K\, g)$ is the unique element of P taking the same values as g on Σ.

Definition 4.3 (**Triangular Mesh**)**.** Given a polyhedral, connected, open susbset $\Omega \subset \mathbb{R}^n$, a **triangular mesh** of $\overline{\Omega}$ is a set $\mathcal{T}_\delta$ of N–simplices $(\mathcal{T}_i)_{1 \leqslant i \leqslant N}$ such that

i. $\mathcal{T}_i \subset \overline{\Omega}$ and $\bigcup\limits_{1 \leqslant i \leqslant N} \mathcal{T}_i = \overline{\Omega}$.

ii. $\mathcal{T}_i \cap \mathcal{T}_j$ is an m–simplex, $0 \leqslant m \leqslant n-1$, whose vertices are vertices of $\mathcal{T}_i$ and $\mathcal{T}_j$.

iii. $\delta = \max\limits_{i=1,\ldots,N} |\mathcal{T}_i|$ is the maximal diameter.

Definition 4.4 (**Triangular Lagrange Finite Element**)**.** Given a triangular mesh $\mathcal{T}_\delta$ of a polyhedral, connected, open subset $\Omega \subset \mathbb{R}^n$, **the triangular Lagrange finite element of order** k, associated to this mesh, is defined by the discrete spaces

$$\mathbb{U}_\delta = \left\{ v \in C(\overline{\Omega}) \quad | \quad v_{|\mathcal{T}_i} \in \mathbb{P}_k \quad \forall\, \mathcal{T}_i \in \mathcal{T}_\delta \right\} \quad \text{and} \quad \mathbb{V}_\delta = \left\{ v \in \mathbb{U}_\delta \quad | \quad v_{|\partial\Omega} = 0 \right\},$$

where $\mathbb{P}_k$ is the space of real polynomials of degree $\leqslant k$.

4.2 Discretization of the Snowflake and of the Boundary of the Snowflake

Property 4.1 (**Discretization of the Boundary of the Snowflake**)**.** *We introduce the sequence of sets of boundary points, denoted by $(V_m)_{m \in \mathbb{N}}$, obtained by means of a uniform discretization of the sequence of boundaries $(\partial \mathfrak{KS}_m)_{m \in \mathbb{N}}$ and such that*

$$\forall\, m \in \mathbb{N}^\star : \quad V_m = V_m^{\mathcal{I}} \cup \mathfrak{h}_1\left(V_m^{\mathcal{I}}\right) \cup \mathfrak{h}_2\left(V_m^{\mathcal{I}}\right) ;$$

where the sequence of sets of vertices $\left(V_m^{\mathcal{I}}\right)_{m \in \mathbb{N}}$ has been introduced in Definition 2.3, on page 7; see also Figure 6, on page 16, for the three first sets, i.e., respectively, V_1, V_2 and V_3.

Property 4.2 (**Discretization of the Snowflake**)**.** *We introduce the sequence of sets of points, denoted by $\left(V_m^{\mathfrak{KS}}\right)_{m \in \mathbb{N}}$ and obtained by means of a uniform discretization mesh of the sets $(\mathfrak{KS}_m)_{m \in \mathbb{N}}$ (Cf. the FEM section 4.3); see Figure 7, on page 16, for the three first sets; namely, $V_1^{\mathfrak{KS}}$, $V_2^{\mathfrak{KS}}$ and $V_3^{\mathfrak{KS}}$.*

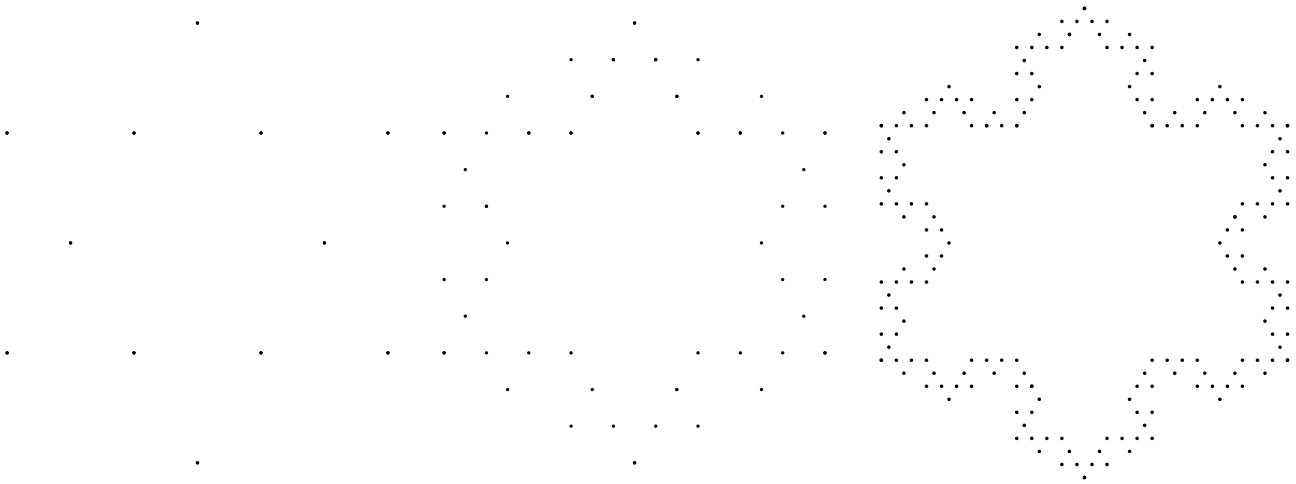

Figure 6 – V_1, V_2 and V_3.

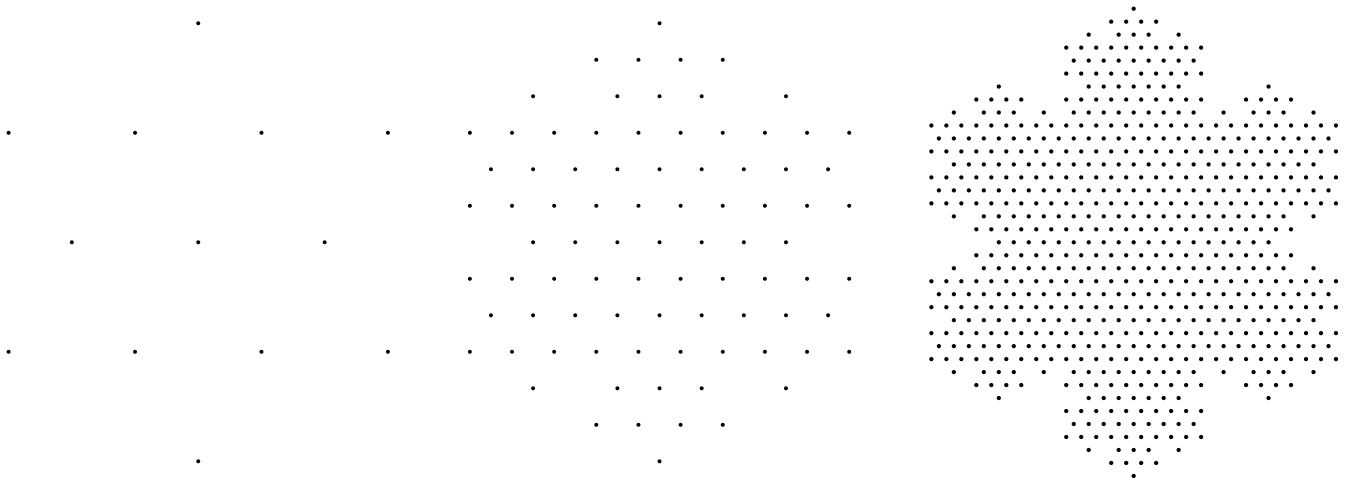

Figure 7 – $V_1^{\mathfrak{KS}}$, $V_2^{\mathfrak{KS}}$ and $V_3^{\mathfrak{KS}}$.

For any $m \in \mathbb{N}^\star$, we can check that every interior point X of $V_m^{\mathfrak{KS}}$ has six neighbors, which are the vertices of an hexagon, where the distance between adajacent vertices is equal to $\delta_m = \mathcal{O}(3^{-m})$; see Figure 8, on page 17. Note that for the points X in $\mathfrak{KS} \setminus V_m^{\mathfrak{KS}}$, we can find a sequence of points $(X_{m,k})_{k\in\mathbb{N}}$ such that, for all $k \in \mathbb{N}$, $X_{m,k} \in V_m^{\mathfrak{KS}}$, with $\lim\limits_{k\to\infty} X_{m,k} = X$.

4.3 Illustration in the Case of the $\mathbb{P}_1$ Finite Element on a Uniform Mesh

As is evoked in the introduction, we herefater work with the sequence of prefractal polygonal approximations $(\mathfrak{KS}_m)_{m\in\mathbb{N}}$ of the Snowflake $\mathfrak{KS}$ introduced in Property 2.5, on page 7, along with the sequence of prefractal approximations $(\partial\mathfrak{KS}_m)_{m\in\mathbb{N}}$ of the boundary $\partial\mathfrak{KS}$, introduced in Property 2.4, on page 7.

Let us start with the following finite set of points:

$$P_1 = (0,-1) \quad ; \quad P_2 = \left(-\frac{\sqrt{3}}{2}, -\frac{1}{2}\right) \quad ; \quad P_3 = \left(-\frac{1}{2\sqrt{3}}, -\frac{1}{2}\right) \quad ; \quad P_4 = \left(\frac{1}{2\sqrt{3}}, -\frac{1}{2}\right) ;$$

$$P_5 = \left(\frac{\sqrt{3}}{2}, -\frac{1}{2}\right) \quad ; \quad P_6 = \left(-\frac{1}{\sqrt{3}}, 0\right) \quad ; \quad P_7 = (0,0) \quad ; \quad P_8 = \left(\frac{1}{\sqrt{3}}, 0\right) \quad ; \quad P_9 = P_1^f = \left(-\frac{\sqrt{3}}{2}, \frac{1}{2}\right)$$

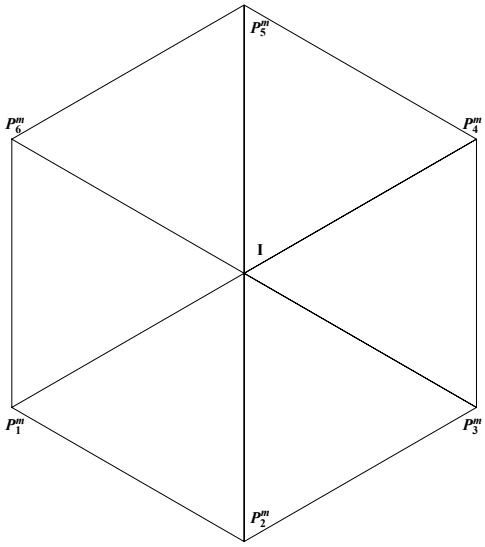

Figure 8 – Hexagonal neighbor of an interior point I.

$$P_{10} = \left(-\frac{1}{2\sqrt{3}}, \frac{1}{2}\right) \quad ; \quad P_{11} = \left(\frac{1}{2\sqrt{3}}, \frac{1}{2}\right) \quad ; \quad P_{12} = P_4^f = \left(\frac{\sqrt{3}}{2}, \frac{1}{2}\right) \quad ; \quad P_{13} = (0, 1) \ ,$$

where the points P_1^f and P_4^f are the respective fixed points of the similarities f_1 and f_4 introduced in Property 2.1, on page 4.

We then obtain the initial triangular mesh $\mathfrak{KS}_1$; see Figure 9, on page 17.

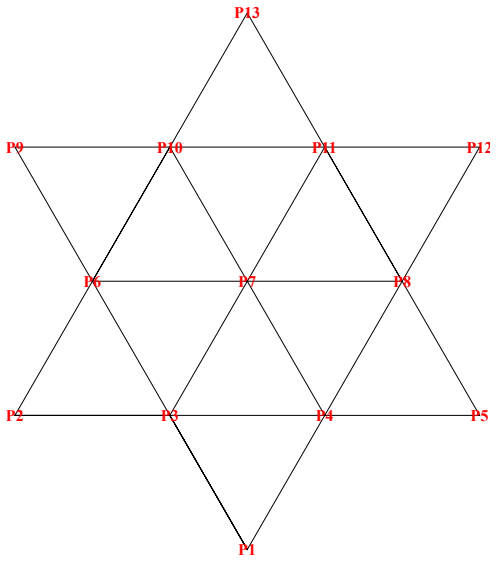

Figure 9 – $\mathfrak{KS}_1$.

This provides us with the first set of vertices $V_1^{\mathfrak{KS}}$.

Next, we use the successive discretization of the Koch Curve to fix the discretization diameter, so we obtain a uniform triangulation mesh of the whole Koch Snowflake.

The Koch Curve discretization sequence $(\mathfrak{KC}_m)_{m\in\mathbb{N}^\star}$ is generated by starting with five points

$$P_9=\left(-\frac{\sqrt{3}}{2},\frac{1}{2}\right)\quad;\quad P_{10}=\left(-\frac{1}{2\sqrt{3}},\frac{1}{2}\right)\quad;\quad P_{13}=(0,1)\quad;\quad P_{11}=\left(\frac{1}{2\sqrt{3}},\frac{1}{2}\right)\quad;\quad P_{12}=\left(\frac{\sqrt{3}}{2},\frac{1}{2}\right)$$

and by using the similarities introduced in Section 2 to obtain the induction relation; namely,

$$\forall\, m\,\in\,\mathbb{N}^\star\quad \mathfrak{KC}_m=\underset{1\leqslant i\leqslant 4}{\cup} f_i\left(\mathfrak{KC}_{m-1}\right)\,.$$

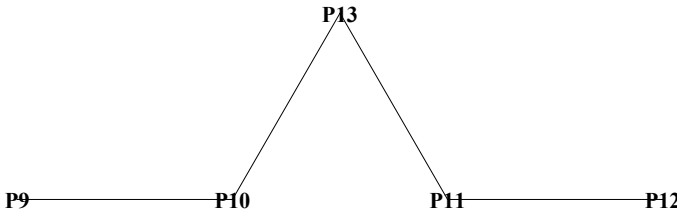

Figure 10 – $\mathfrak{KC}_1$.

By using the two rotations $\mathfrak{h}_1$ and $\mathfrak{h}_2$, we also obtain the sequence of boundary points $(V_m)_{m\in\mathbb{N}}$; see figure 6, on page 16.

By using a uniform diameter, i.e., for any $m\,\in\,\mathbb{N}^\star$, $\delta_m=\dfrac{1}{3^m}$, we obtain the points of the discretization of the Snowflake $\left(V_m^{\mathfrak{KS}}\right)_{m\in\mathbb{N}}$; see Figure 7, on page 16.

Proposition 4.3 (**[LNRG96]**). *Given an integer $m\,\in\,\mathbb{N}$, let us denote respectively by $\mathcal{N}'_m$, the number of vertices of the triangulation of the boundary and by $\mathcal{N}(\mathfrak{KS})_m$ and $\mathcal{N}_m$, the numbers of triangles and vertices of the Snowflake triangulation. We have that*

$$\mathcal{N}'_1=12\quad,\quad \mathcal{N}(\mathfrak{KS})_1=12,\quad \mathcal{N}_1=13\,,$$

and, for any strictly positive integer m:

$$\mathcal{N}'_m=3\times 4^m \tag{7}$$

$$\mathcal{N}(\mathfrak{KS})_m=\left(9^m+\frac{3}{5}\left(9^m-4^m\right)\right) \tag{8}$$

$$\mathcal{N}_m=\frac{\mathcal{N}'_m+\mathcal{N}(\mathfrak{KS})_m}{2}+1\,. \tag{9}$$

First, given $m\,\in\,\mathbb{N}^\star$, we compute the values of the respective two–dimensional Lebesgue measures $\left(\mu_{\mathcal{L}}\left(\mathcal{T}_i^m\right)\right)_{1\leqslant i\leqslant\mathcal{N}(\mathfrak{KS})_m}$ of the m^{th}–order mesh triangles $(\mathcal{T}_i^m)_{1\leqslant i\leqslant\mathcal{N}(\mathfrak{KS})_m}$; see Definition 4.3, on page 15). Namely,

$$\mu_{\mathcal{L}}\left(\mathcal{T}^0\right)=\mu_{\mathcal{L}}\left(P_2P_5P_{13}\right)=\frac{1}{2}\left(\frac{\sqrt{3}}{2}+\frac{\sqrt{3}}{2}\right)\times\left(1+\frac{1}{2}\right)=\frac{3\sqrt{3}}{4}$$

and

$$\forall\, m\,\in\,\mathbb{N}^\star\,:\quad \mu_{\mathcal{L}}\left(\mathcal{T}_i^m\right)=\frac{\mu_{\mathcal{L}}\left(\mathcal{T}^0\right)}{9^m}\,.$$

Given $m \in \mathbb{N}^\star$ and the discretization points of $V_m^{\mathfrak{KG}}$, let $\mathcal{T}_l^m = P_a P_b P_c$, $1 \leqslant l \leqslant \mathcal{N}(\mathfrak{KG})_m$ be a mesh triangle. We then define the associated **barycentric coordinates** λ_i^m, with $i \in \{a, b, c\}$ (see, for instance, the book [Luc04]), such that, for all $M = (x, y) \in \mathbb{R}^2$,

$$\sum_{i \in \{a,b,c\}} \lambda_i^m(M) = 1 \quad \text{and} \quad \sum_{i \in \{a,b,c\}} P_i \lambda_i^m(M) = M\,.$$

For the initial triangle $\mathcal{T}^0 = P_2 P_5 P_{13}$, we compute

$$\nabla\lambda_2^0(M) = \begin{pmatrix} -\frac{1}{\sqrt{3}} \\ -\frac{1}{3} \end{pmatrix} \quad , \quad \nabla\lambda_5^0(M) = \begin{pmatrix} \frac{1}{\sqrt{3}} \\ -\frac{1}{3} \end{pmatrix} \quad , \quad \nabla\lambda_{13}^0(M) = \begin{pmatrix} 0 \\ \frac{2}{3} \end{pmatrix}.$$

$$\int_{\mathcal{T}_0} |\nabla\lambda_2^0|^2\,dx = \frac{1}{\sqrt{3}} \quad , \quad \int_{\mathcal{T}_0} |\nabla\lambda_5^0|^2\,dx = \frac{1}{\sqrt{3}} \quad , \quad \int_{\mathcal{T}_0} |\nabla\lambda_{13}^0|^2\,dx = \frac{1}{\sqrt{3}}$$
$$\int_{\mathcal{T}_0} \nabla\lambda_2^0 \nabla\lambda_5^0\,dx = -\frac{\sqrt{3}}{6} \quad , \quad \int_{\mathcal{T}_0} \nabla\lambda_2^0 \nabla\lambda_{13}^0\,dx = -\frac{\sqrt{3}}{6} \quad , \quad \int_{\mathcal{T}_0} \nabla\lambda_5^0 \nabla\lambda_{13}^0\,dx = -\frac{\sqrt{3}}{6}\,.$$

More generally, given $m \in \mathbb{N}^\star$ and the set $\mathfrak{KG}_m$, we consider a mesh triangle $\mathcal{T}_l^m = P_i P_j P_k$, $1 \leqslant l \leqslant \mathcal{N}(\mathfrak{KG})_m$, for some vertices $P_i = (x_i, y_i)$, $P_j = (x_j, y_j)$, $P_k = (x_k, y_k)$. The barycentric coordinates are then given by:

$$\lambda_i^m(M) = \frac{1}{2\,\mu_{\mathcal{L}}\left(\mathcal{T}_l^m\right)} \left(X(y_j - y_k) + Y(x_k - x_j) + x_j y_k - y_j x_k\right);$$
$$\lambda_j^m(M) = \frac{1}{2\,\mu_{\mathcal{L}}\left(\mathcal{T}_l^m\right)} \left(X(y_k - y_i) + Y(x_i - x_k) + x_k y_i - y_k x_i\right);$$
$$\lambda_k^m(M) = \frac{1}{2\,\mu_{\mathcal{L}}\left(\mathcal{T}_l^m\right)} \left(X(y_i - y_j) + Y(x_j - x_i) + x_i y_j - y_i x_j\right);$$

the associated gradients are themselves given by

$$\nabla\lambda_i^m(M) = \frac{1}{2\,\mu_{\mathcal{L}}\left(\mathcal{T}_l^m\right)} \begin{pmatrix} y_j - y_k \\ x_k - x_j \end{pmatrix} = 3^m \nabla\lambda_2^0(M)\,;$$
$$\nabla\lambda_j^m(M) = \frac{1}{2\,\mu_{\mathcal{L}}\left(\mathcal{T}_l^m\right)} \begin{pmatrix} y_k - y_i \\ x_i - x_k \end{pmatrix} = 3^m \nabla\lambda_5^0(M)\,;$$
$$\nabla\lambda_k^m(M) = \frac{1}{2\,\mu_{\mathcal{L}}\left(\mathcal{T}_l^m\right)} \begin{pmatrix} y_i - y_j \\ x_j - x_i \end{pmatrix} = 3^m \nabla\lambda_{13}^0(M)\,.$$

We then deduce that

$$\int_{\mathcal{T}_l^m} |\nabla\lambda_i^m|^2\,dx = \int_{\mathcal{T}_l^m} |\nabla\lambda_j^m|^2\,dx = \int_{\mathcal{T}_l^m} |\nabla\lambda_k^m|^2\,dx = 9^{-m} \int_{\mathcal{T}^0} 9^m |\nabla\lambda_2^0|^2\,dx = \frac{1}{\sqrt{3}}\,;$$

$$\int_{\mathcal{T}_l^m} \nabla\lambda_i^m \nabla\lambda_j^m\,dx = \int_{\mathcal{T}_l^m} \nabla\lambda_i^m \nabla\lambda_k^m\,dx = \int_{\mathcal{T}_l^m} \nabla\lambda_j^m \nabla\lambda_k^m\,dx = 9^{-m} \int_{\mathcal{T}^0} 9^m \nabla\lambda_2^0 \nabla\lambda_5^0\,dx = -\frac{\sqrt{3}}{6}\,.$$

Now, we can compute the cross product involving the local basis functions. The function h is taken as constant on every mesh triangle $\mathcal{T}_l^m$ and given a local basis function e_i (see Definition 4.2, on page 15) associated to a point P_i, we denote by $l(i)$ the triangle number l containing vertex P_i, and by $l(i, j)$ the triangle number l adjacent to edge $P_i P_j$, $i \neq j$. The following two configurations may occur:

1. The point P_i is an interior point, in which case we have that

$$\int_{\mathfrak{KS}} h\,|\nabla e_i|^2\,dx = \sum_{l=1}^{6} h_{l(i)} \int_{\mathcal{T}_l^m} |\nabla \lambda_i|^2\,dx = \left(\sum_{l=1}^{6} h_{l(i)}\right)\,\frac{1}{\sqrt{3}}\,;$$

$$\int_{\mathfrak{KS}} h\,\nabla e_i \nabla e_j\,dx = \begin{cases} (h_{1(i,j)} + h_{2(i,j)}) \displaystyle\int_{\mathcal{T}_l^m} \nabla\lambda_i \nabla\lambda_j\,dx = (h_{1(i,j)} + h_{2(i,j)}) \left(\frac{-\sqrt{3}}{6}\right), \\ 0\,, \text{ if } \mathrm{Supp}(e_i) \cap \mathrm{Supp}(e_j) = \emptyset\,. \end{cases}$$

2. The point P_i is a boundary point, two situations have then to be considered:

   (a) The point P_i has two adjacent vertices, in which case

$$\int_{\mathfrak{KS}} h\,|\nabla e_i|^2\,dx = h_l \int_{\mathcal{T}_l^m} |\nabla \lambda_i|^2\,dx = \frac{h_l}{\sqrt{3}}\,;$$

$$\int_{\mathfrak{KS}} h\,\nabla e_i \nabla e_j\,dx = \begin{cases} h_l \displaystyle\int_{\mathcal{T}_l^m} \nabla\lambda_i \nabla\lambda_j\,dx = h_l \left(\frac{-\sqrt{3}}{6}\right) \\ 0 \text{ if } \mathrm{Supp}(e_i) \cap \mathrm{Supp}(e_j) = \emptyset\,. \end{cases}$$

   (b) The point P_i has five adjacent vertices, in which case

$$\int_{\mathfrak{KS}} h\,|\nabla e_i|^2\,dx = \sum_{l=1}^{5} h_{l(i)} \int_{\mathcal{T}_l^m} |\nabla \lambda_i|^2\,dx = \left(\sum_{k=1}^{5} h_k\right) \frac{1}{\sqrt{3}}$$

$$\int_{\mathfrak{KS}} h\,\nabla e_i \nabla e_j\,dx = \begin{cases} (h_1(i,j) + h_2(i,j)) \displaystyle\int_{\mathcal{T}_l^m} \nabla\lambda_i \nabla\lambda_j\,dx = (h_k + h_l) \left(\frac{-\sqrt{3}}{6}\right) \\ \qquad\qquad\qquad\qquad\qquad\qquad \text{if } P_j \text{ is an interior point,} \\ h_l \displaystyle\int_{\mathcal{T}_l^m} \nabla\lambda_i \nabla\lambda_j\,dx = h_l \left(\frac{-\sqrt{3}}{6}\right) \text{ if } P_j \text{ is a boundary point,} \\ 0 \text{ if } \mathrm{Supp}(e_i) \cap \mathrm{Supp}(e_j) = \emptyset\,. \end{cases}$$

4.4 Convergence and Error Estimates

Given an integer $m \in \mathbb{N}$, we consider $\mathfrak{KS}_m$ as the uniform triangulation of the Koch snowflake at the order m and $\mathring{\mathfrak{KS}}_m$ its interior. The main object of this section is to estimate the convergence of the finite element method at the order m. We adopt the methodology of [RJM04].

First, we observe that

$$\mathfrak{KS}_m = \bigcup_i \mathcal{T}_i^m \subset \mathfrak{KS}\,.$$

For any $m \in \mathbb{N}^\star$, we respectively denote by δ_m and ρ_m the diameter of the mesh triangles and their roundness (incircle diameter).

The triangulation is regular, since

$$\delta_m = \frac{\sqrt{3}}{3^m} \quad , \quad \rho_m = \frac{1}{3^m} \quad , \quad \frac{\delta_m}{\rho_m} = \sqrt{3}, \quad \lim_{m\to\infty} \delta_m = 0\,,$$

and using the fact that $\mathfrak{KS}$ is a John domain we get the regularity (see [Pom92] page 107 for an alternative definition)

$$\forall\, X \,\in\, \partial\mathfrak{KS}_m \cap \mathcal{T}_l^m \,:\quad d_{eucl}(X, \partial\mathfrak{KS}) \leqslant C_0\, \delta_m\,. \tag{10}$$

Let us consider the discrete space

$$\mathbb{V}_{\delta_m} = \left\{ v \in C(\mathfrak{KS}_m);\quad v_{|\mathcal{T}_l^m} \,\in\, \mathbb{P}_k \quad \forall \mathcal{T}_l^m \in \mathcal{T}_{\delta_m},\quad v_{|\partial\mathfrak{KS}_m} = 0 \right\}, \tag{11}$$

and the natural extension by zero on the following unresolved features

$$\widetilde{\mathbb{V}}_{\delta_m} = \left\{ \tilde{v} \in C(\mathfrak{KS});\quad \tilde{v}_{|\mathring{\mathfrak{KS}}_m} \in \mathbb{V}_{\delta_m},\quad \tilde{v}_{|\mathring{\mathfrak{KS}}\setminus\mathring{\mathfrak{KS}}_m} = 0 \right\}. \tag{12}$$

Now, let us consider the solution $\tilde{u}_m$ of the variational Dirichlet problem ($\mathcal{D}ir_{var}$) given in equation (6) of Section 3:

$$\forall\, \tilde{v}_m \,\in\, \widetilde{\mathbb{V}}_{\delta_m},\qquad a(\tilde{u}_m, \tilde{v}_m) = L(\tilde{v}_m)\,.$$

Thanks to the symmetry of the bilinear form, we have that

$$\|u - \tilde{u}_m\|_{H_0^1(\mathring{\mathfrak{KS}}_m)} \leqslant \sqrt{\frac{(C+1)\, h_{max}}{h_{min}}} \inf_{\tilde{v}_m \in \widetilde{\mathbb{V}}_{\delta_m}} \|u - \tilde{v}_m\|_{H_0^1(\mathring{\mathfrak{KS}}_m)}\,.$$

(C is the Poincaré constant introduced in Theorem 2.9, on page 11.)

Indeed, since $\tilde{v}_m - \tilde{u}_m \,\in\, H_0^1(\mathring{\mathfrak{KS}}_m)$ is an admissible function, we have that

$$\forall\, \tilde{v}_m \,\in\, \widetilde{\mathbb{V}}_{\delta_m},\qquad a(u, \tilde{v}_m - \tilde{u}_m) = L(\tilde{v}_m - \tilde{u}_m)\,,$$

we have that

$$\forall\, \tilde{v}_m \,\in\, \widetilde{\mathbb{V}}_{\delta_m},\qquad a(u - \tilde{u}_m, \tilde{v}_m - \tilde{u}_m) = 0\,, \tag{13}$$

or, equivalently,

$$\forall\, \tilde{v}_m \,\in\, \widetilde{\mathbb{V}}_{\delta_m},\qquad a(u - \tilde{u}_m, u - \tilde{u}_m) = a(u - \tilde{u}_m, u - \tilde{v}_m)\,. \tag{14}$$

By using the coercitivity of the bilinear form $a(.,.)$, we obtain that

$$\|u - \tilde{u}_m\|_{H_0^1(\mathring{\mathfrak{KS}}_m)} \leqslant \frac{(C+1)\, h_{max}}{h_{min}}\, \|u - \tilde{v}_m\|_{H_0^1(\mathring{\mathfrak{KS}}_m)}\,.$$

From this result, along with relation (13) just above, we deduce that $\tilde{u}_m$ is the orthogonal projection of u with respect to the norm $\|.\|_a$ (or, equivalently, the scalar product associated to a on $H_0^1(\mathring{\mathfrak{KS}}_m)$; i.e.,

$$\forall\, \tilde{v}_m \,\in\, \widetilde{\mathbb{V}}_{\delta_m} \,:\quad \|u - \tilde{u}_m\|_a^2 \leqslant \|u - \tilde{v}_m\|_a^2\,.$$

We then use the regularity of the bilinear form $a(.,.)$ on this expression; namely,

$$h_{max}\, \|u - \tilde{u}_m\|^2_{H_0^1(\mathring{\mathfrak{KS}}_m)} \leqslant \frac{h_{min}}{C+1}\, \|u - \tilde{v}_m\|^2_{H_0^1(\mathring{\mathfrak{KS}}_m)}\,. \tag{15}$$

to finally obtain that

$$\|u-\tilde{u}_m\|_{H_0^1(\mathring{\mathfrak{KS}}_m)} \leqslant \sqrt{\frac{(C+1)\,h_{max}}{h_{min}}} \inf_{\tilde{v}_m\in\widetilde{\mathbb{V}}_{\delta_m}} \|u-\tilde{v}_m\|_{H_0^1(\mathring{\mathfrak{KS}}_m)}\ . \tag{16}$$

and using the equivalence of the two norms in H_0^1

$$|u-\tilde{u}_m|_{H_0^1(\mathring{\mathfrak{KS}}_m)} \lesssim \inf_{\tilde{v}_m\in\widetilde{\mathbb{V}}_{\delta_m}} |u-\tilde{v}_m|_{H_0^1(\mathring{\mathfrak{KS}}_m)}\,. \tag{17}$$

which becomes

$$|u-u_m|_{H_0^1(\mathring{\mathfrak{KS}}_m)} \lesssim \inf_{v_m\in\mathbb{V}_{\delta_m}} |u-v_m|_{H_0^1(\mathring{\mathfrak{KS}}_m)}\,. \tag{18}$$

We now have to take into account the fact that (see figures 11 and 12)

$$|u-\tilde{u}_m|_{H_0^1(\mathring{\mathfrak{KS}})} = \left(|u-u_m|^2_{H_0^1(\mathring{\mathfrak{KS}}_m)} + |u|^2_{H_0^1(\mathring{\mathfrak{KS}}\setminus\mathring{\mathfrak{KS}}_m)}\right)^{\frac{1}{2}}\ . \tag{19}$$

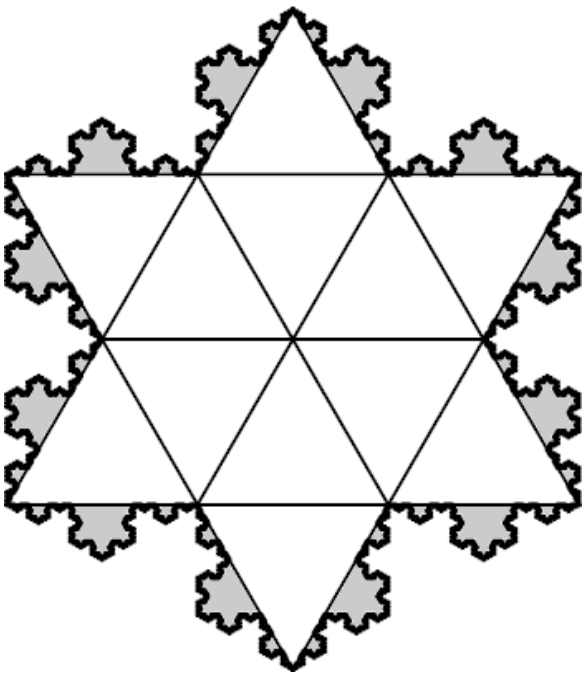

Figure 11 – The open set $\mathring{\mathfrak{KS}}\setminus\mathring{\mathfrak{KS}}_m$ for $m=1$.

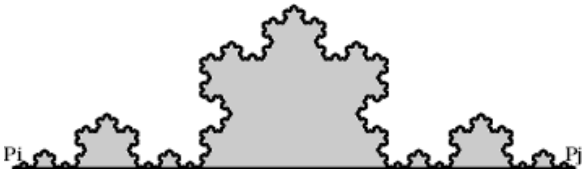

Figure 12 – The open set O_i of $\mathring{\mathfrak{KS}}\setminus\mathring{\mathfrak{KS}}_m$ delimited by $[P_i,P_j]$.

Now, given $m\in\mathbb{N}$, let us consider the interpolation operator π_m on $\mathring{\mathfrak{KS}}_m$, which, to any continuous function on $\mathfrak{KS}$ associates the continuous function $\pi_m u$ on $\mathfrak{KS}_m$, such that, for any triangle mesh $\mathcal{T}_l^m\in\mathcal{T}_{\delta_m}$, the restriction $(\pi_m u)_{|\mathcal{T}_l^m}$ is the Lagrange interpolation on $\mathcal{T}_l^m$ and which is identically equal to zero on the vertices of $\partial\mathfrak{KS}_m$.

We will first establish a general result for h in L^∞ on the regular approximation domain $\mathfrak{KS}_m$. Remark that $W^2_\infty(\mathring{\mathfrak{KS}})\cap H_0^1(\mathring{\mathfrak{KS}})$ is dense in $H_0^1(\mathring{\mathfrak{KS}})$ (contains $\mathcal{D}(\mathring{\mathfrak{KS}})$). Then we decompose the error

by choosing $v \in W^2_\infty(\mathring{\mathfrak{KS}}) \cap H^1_0(\mathring{\mathfrak{KS}})$ and $m \in \mathbb{N}$ such that, $\forall \varepsilon > 0$

$$\begin{aligned}\|u - \pi_m v\|_{H^1(\mathring{\mathfrak{KS}}_m)} &\leqslant \|u - v\|_{H^1(\mathring{\mathfrak{KS}}_m)} + \|v - \pi_m v\|_{H^1(\mathring{\mathfrak{KS}}_m)} \\ &\lesssim \|u - v\|_{H^1(\mathring{\mathfrak{KS}}_m)} + \delta_m \|v\|_{W^2_\infty(\mathring{\mathfrak{KS}}_m)} \\ &\lesssim \|u - v\|_{H^1(\mathring{\mathfrak{KS}})} + \delta_m \|v\|_{W^2_\infty(\mathring{\mathfrak{KS}})} \\ &\leqslant \frac{\varepsilon}{2} + \frac{\varepsilon}{2} = \varepsilon\end{aligned}$$

where we used the density of $W^2_\infty(\mathring{\mathfrak{KS}}) \cap H^1_0(\mathring{\mathfrak{KS}})$ in $H^1_0(\mathring{\mathfrak{KS}})$, and we applied theorem 3.1.6 in [Cia02], page 124, on the regular domain $\mathring{\mathfrak{KS}}_m$ to get the upper bound of $\|v - \pi_m v\|_{H^1(\mathring{\mathfrak{KS}}_m)}$, then we extended the norm to the whole domain $\mathring{\mathfrak{KS}}$ by the choice of v.

If we analyze the second part of the error $\|u\|_{H^1_0(\mathring{\mathfrak{KS}} \setminus \mathring{\mathfrak{KS}}_m)}$, given that $u \in H^1_0(\mathring{\mathfrak{KS}})$, one can employ the dominated convergence theorem. Specifically, note that the inequalities

$$\mathbf{1}_{\mathring{\mathfrak{KS}} \setminus \mathring{\mathfrak{KS}}_m} |u|^2 \leqslant |u|^2 \quad \text{and} \quad \mathbf{1}_{\mathring{\mathfrak{KS}} \setminus \mathring{\mathfrak{KS}}_m} |\nabla u|^2 \leqslant |\nabla u|^2$$

hold for every m, where $\mathbf{1}_{\mathring{\mathfrak{KS}} \setminus \mathring{\mathfrak{KS}}_m}$ is the characteristic function of the set $\mathring{\mathfrak{KS}} \setminus \mathring{\mathfrak{KS}}_m$. Since $|u|^2$ and $|\nabla u|^2$ are integrable over $\mathring{\mathfrak{KS}}$, the shrinking measure of $\mathring{\mathfrak{KS}} \setminus \mathring{\mathfrak{KS}}_m$ as $m \to \infty$ ensures that

$$\lim_{m \to \infty} \|u\|_{H^1(\mathring{\mathfrak{KS}} \setminus \mathring{\mathfrak{KS}}_m)} = 0. \tag{20}$$

We have proved the following:

Proposition 4.4. *Let $f \in L^2(\mathring{\mathfrak{KS}})$ and $h \in L^\infty(\mathring{\mathfrak{KS}})$ then*

$$\lim_{m \to \infty} \|u - \tilde{u}_m\|_{H^1(\mathring{\mathfrak{KS}})} = 0 \tag{21}$$

We now proceed to compute the convergence order of the finite element method applied to our elliptic problem. This computation, however, necessitates imposing additional restrictions on h. We begin recalling the following lemma:

Lemma 4.5 ([RJM04]). *Given $m \in \mathbb{N}^\star$, let $\mathcal{T}_l^m$ be a mesh. We denote by $k \geqslant 1$ the interpolation order. There exists a real constant $C > 0$, depending only on k and m, such that, for all $0 \leqslant n \leqslant k+1$ and for each $v \in H^{k+1}(\mathcal{T}_l^m)$,*

$$|v - \pi_m v|_{H^n_0(\mathcal{T}_l^m)} \leqslant C \, \frac{\delta_m^{k+1}}{\rho_m^n} \, |v|_{H^{k+1}_0(\mathcal{T}_l^m)} \, . \tag{22}$$

- **The case $k = 1$:**

  In that case, the function $\pi_m u$ belongs to $\mathbb{V}_{\delta_m}$. We can use We have the following lemma 4.5 to deduce the following result:

  Lemma 4.6. *Let us assume that $k = 1$. Given $m \in \mathbb{N}^\star$, we have, for every function $h \in C^1(\mathfrak{KS})$ and $f \in L^2(\mathring{\mathfrak{KS}})$,*

$$\inf_{v_m \in \mathbb{V}_{\delta_m}} |u - v_m|_{H^1_0(\mathring{\mathfrak{KS}}_m)} \lesssim \delta_m \left(\|f\|_{L^2(\mathring{\mathfrak{KS}})} + \|u\|_{L^2(\mathring{\mathfrak{KS}})} \right) . \tag{23}$$

Proof.
Using lemma 4.5 and theorem 3.2:

$$\inf_{v_m\in\mathbb{V}_{\delta_m}} |u-v_m|_{H_0^1(\mathring{\mathfrak{KS}}_m)} \lesssim |u-\pi_m u|_{H_0^1(\mathring{\mathfrak{KS}}_m)} \lesssim \delta_m\,|u|_{H_0^2(\mathring{\mathfrak{KS}}_m)} \lesssim \delta_m\,\|u\|_{H^2(\mathring{\mathfrak{KS}}_m)}$$
$$\lesssim \delta_m\left(\|f\|_{L^2(\mathring{\mathfrak{KS}})} + \|u\|_{L^2(\mathring{\mathfrak{KS}})}\right).$$

□

- **The case $k \geqslant 2$:**

In that case, the function $\pi_m u$ does not belong to $\mathbb{V}_{\delta_m}$ ($\pi_m u$ isn't null on $\partial\mathfrak{KS}_m$). We need to prove the following lemma:

Lemma 4.7. *Let us assume that $k \geqslant 2$. Given $m \in \mathbb{N}^\star$, we have, for every function $h \in C^3(\mathfrak{KS})$ and $f \in H^2(\mathring{\mathfrak{KS}})$, that*

$$\inf_{v_m\in\mathbb{V}_{\delta_m}} |u-v_m|_{H_0^1(\mathring{\mathfrak{KS}}_m)} \lesssim \delta_m^2\,\left(\|f\|_{H^2(\mathring{\mathfrak{KS}})} + \|u\|_{L^2(\mathring{\mathfrak{KS}})}\right). \tag{24}$$

Proof. We give here an adaptation of the proof which can be found in the book [RJM04]. Let π_m^0 be the interpolation function such that $\pi_m^0 u \in \mathbb{V}_{\delta_m}$. The support of $\pi_m u - \pi_m^0 u$ is the set of boundary triangles $\mathcal{T}_l^m \cap \partial\mathcal{T}_{\delta_m} \neq \emptyset$. We can use the triangle inequality; namely,

$$\inf_{v_m\in\mathbb{V}_{\delta_m}} |u-v_m|_{H_0^1(\mathring{\mathfrak{KS}}_m)} \leqslant |u-\pi_m^0 u|_{H_0^1(\mathring{\mathfrak{KS}}_m)} \leqslant |u-\pi_m u|_{H_0^1(\mathring{\mathfrak{KS}}_m)} + |\pi_m u-\pi_m^0 u|_{H_0^1(\mathring{\mathfrak{KS}}_m)}.$$

On the one hand, thanks to Lemma 4.5, on page 23, we have that

$$|u-\pi_m u|_{H_0^1(\mathcal{T}_l^m)} \lesssim \frac{\delta_m^4}{\rho_m}\,|u|_{H_0^4(\mathcal{T}_l^m)} \lesssim \frac{\delta_m^4}{\rho_m}\,\|u\|_{H^4(\mathcal{T}_l^m)}.$$

We thus use theorem 3.2 to deduce that

$$|u-\pi_m u|_{H_0^1(\mathring{\mathfrak{KS}}_m)} \lesssim \frac{\delta_m^4}{\rho_m}\,\|u\|_{H^4(\mathring{\mathfrak{KS}}_m)} \lesssim \delta_m^3\,\left(\|f\|_{H^2(\mathring{\mathfrak{KS}})} + \|u\|_{L^2(\mathring{\mathfrak{KS}})}\right).$$

On the other hand, let $\mathcal{T}_l^m = P_iP_jP_k$ be a boundary mesh triangle, such that $\{P_i, P_j\} \in \partial\mathfrak{KS}$. We set $P_{ij} = \dfrac{P_i+P_j}{2}$ and denote by $P_{ij\star}$ the intersection point of the bisector of the line segment $[P_i, P_j]$ with $\partial\mathfrak{KS}$; see Figure 13 just below (P_{ij} could be any interpolation point on the segment $[P_i, P_j]$).

Given the basis function e_l associated with $\mathcal{T}_l^m$, we deduce that

$$(\pi_m u - \pi_m^0 u)_{|\mathcal{T}_l^m} = u(P_{ij})e_l.$$

Recall that any point P_α in the segment $[P_i, P_j]$ could be written as $P_\alpha = \alpha\,P_j + (1-\alpha)\,P_i$ for $0 \leqslant \alpha \leqslant 1$. Define $\hat{u}(\alpha) = u(\alpha\,P_j + (1-\alpha)\,P_i)$. By using Taylor-Lagrange formula, for some $0 \leqslant \alpha_1 \leqslant \alpha$ and $\alpha \leqslant \alpha_2 \leqslant 1$,

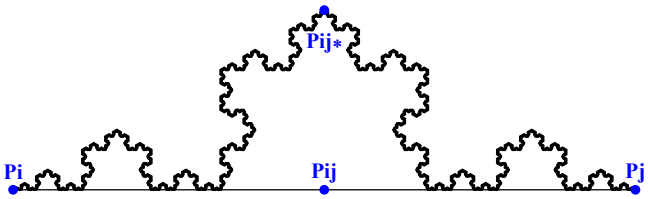

Figure 13 – The edge $\{P_i, P_j\} \in \partial\mathfrak{KS}$ of the boundary triangle $\mathcal{T}_l^m$.

$$\begin{aligned}
\hat{u}(0) = u(P_i) &= \hat{u}(\alpha) - \alpha\,\hat{u}'(\alpha) + \frac{\alpha^2}{2}\hat{u}''(c_1) \\
&= u(P_\alpha) - \alpha\,\nabla u(P_\alpha)\cdot(P_j - P_i) + \frac{\alpha^2}{2}(P_j - P_i)\cdot D^2u(P_{\alpha_1})\cdot(P_j - P_i) \\
&= u(P_\alpha) - \alpha\,\delta_m|\nabla u(P_\alpha)| + \frac{\alpha^2\delta_m^2}{2}|D^2u(P_{\alpha_1})| \\
\hat{u}(1) = u(P_j) &= u(P_\alpha) + \alpha\,\delta_m|\nabla u(P_\alpha)| + \frac{(1-\alpha)^2\delta_m^2}{2}|D^2u(P_{\alpha_2})|
\end{aligned}$$

Summing the two identities for $\alpha = \dfrac{1}{2}$, along with the continuous injection of Sobolev space $H^2(\mathring{\mathcal{T}}_l^m)$ in $C^0(\mathcal{T}_l^m)$ (see for example [Bre99]), we obtain that

$$|u(P_{ij})| = \left|-\frac{\delta_m^2}{16}|D^2u(c_1) + D^2u(c_2)|\right| \leqslant \frac{\delta_m^2}{8}\max_{0\leqslant\alpha\leqslant1}\left|D^2u(P_\alpha)\right| \lesssim \delta_m^2\,\|D^2u\|_{H^2(\mathring{\mathfrak{KS}}_m)}\,.$$

Consequently,

$$\forall\,\mathcal{T}_l^m \in \partial\mathfrak{KS}_m : \quad |\pi_m u - \pi_m^0 u|_{H_0^1(\mathcal{T}_l^m)} \lesssim \delta_m^2\,\|D^2u\|_{H^2(\mathring{\mathfrak{KS}}_m)}\,.$$

In the end, using theorem 3.2, we have that

$$\begin{aligned}
|\pi_m u - \pi_m^0 u|_{H_0^1(\mathring{\mathfrak{KS}}_m)} &= \left(\sum_{\mathcal{T}_l^m\,\in\,\partial\mathfrak{KS}_m}|\pi_m u - \pi_m^0 u|^2_{H_0^1(\mathcal{T}_l^m)}\right)^{\frac{1}{2}} \\
&\lesssim \delta_m^{\frac{3}{2}}\,\|D^2u\|_{H^2(\mathring{\mathfrak{KS}}_m)} \\
&\lesssim \delta_m^{\frac{3}{2}}\,\|u\|_{H^4(\mathring{\mathfrak{KS}}_m)} \\
&\lesssim \delta_m^{\frac{3}{2}}\left(\|f\|_{H^2(\mathring{\mathfrak{KS}})} + \|u\|_{L^2(\mathring{\mathfrak{KS}})}\right)\,.
\end{aligned}$$

□

Now, by combining those results with Inequality (18), on page 22, we obtain the following theorem about the convergence of the finite element method:

Proposition 4.8. *Denote by k the interpolation order, introduced in lemma 4.5, and by f the force term in the right hand side of the problem $(\mathcal{P}_{\mathcal{H}})$. Given $m \in \mathbb{N}^{\star}$, we have that*

$$\forall\, f \in L^2(\mathring{\mathfrak{KS}}) \text{ and } \forall\, h \in C^1(\mathfrak{KS}): \quad |u-\tilde{u}_m|_{H_0^1(\mathring{\mathfrak{KS}}_m)} \lesssim \delta_m \left(\|f\|_{L^2(\mathring{\mathfrak{KS}})} + \|u\|_{L^2(\mathring{\mathfrak{KS}})} \right) \quad \text{for } k=1\ , \tag{25}$$

$$\forall\, f \in H^2(\mathring{\mathfrak{KS}}) \text{ and } \forall\, h \in C^3(\mathfrak{KS}): \quad |u-\tilde{u}_m|_{H_0^1(\mathring{\mathfrak{KS}}_m)} \lesssim \delta_m^{\frac{3}{2}} \left(\|f\|_{H^2(\mathring{\mathfrak{KS}})} + \|u\|_{L^2(\mathring{\mathfrak{KS}})} \right) \quad \text{for } k \geqslant 2\ . \tag{26}$$

We now merge Propositions 4.4 and 4.8 into a unified theorem:

Theorem 4.9 (**Convergence of the FEM Method**). *We recall that k denotes the interpolation order, introduced in lemma 4.5, on page 23, f is the force term and h is the membrane thickness of the problem $(\mathcal{P}_{\mathcal{H}})$ on page 13. Given $m \in \mathbb{N}^{\star}$, the following results hold:*

1. *If $f \in L^2(\mathring{\mathfrak{KS}})$ and $h \in L^{\infty}(\mathring{\mathfrak{KS}})$, then:*

$$\lim_{m\to\infty} \|u-\tilde{u}_m\|_{H^1(\mathring{\mathfrak{KS}})} = 0 \tag{27}$$

2. *In addition:*

   (a) *If $f \in L^2(\mathring{\mathfrak{KS}})$ and $h \in C^1(\mathfrak{KS})$, then:*

$$|u-\tilde{u}_m|_{H_0^1(\mathring{\mathfrak{KS}}_m)} \lesssim \delta_m \left(\|f\|_{L^2(\mathring{\mathfrak{KS}})} + \|u\|_{L^2(\mathring{\mathfrak{KS}})} \right) \qquad \text{for } k=1\ , \tag{28}$$

   (b) *If $f \in H^2(\mathring{\mathfrak{KS}})$ and $h \in C^3(\mathfrak{KS})$, then:*

$$|u-\tilde{u}_m|_{H_0^1(\mathring{\mathfrak{KS}}_m)} \lesssim \delta_m^{\frac{3}{2}} \left(\|f\|_{H^2(\mathring{\mathfrak{KS}})} + \|u\|_{L^2(\mathring{\mathfrak{KS}})} \right) \qquad \text{for } k \geqslant 2\ . \tag{29}$$

One could observe that increasing the interpolation order does not necessarily improve the convergence speed. This can be attributed to the loss of regularity caused by the fractal nature of the boundary.

4.5 Numerical Results

In this section, we ilustrate the numerical solution of the Dirichlet membrane problem by means of the finite element method, namely,

$$(\mathcal{P}_{\mathcal{H}}) \quad \begin{cases} -\mathrm{div}\,(h\nabla u) &= f \quad \text{in } \mathring{\mathfrak{KS}}\,, \\ u &= 0 \quad \text{in } \partial\mathfrak{KS}\,, \end{cases}$$

for $h=1$ and $f(M)=e^{-\left(x^2+y^2\right)}$. The solutions are generated by using the package NDSolve‘FEM‘ of Mathematica; see Figure 14, on page 27, for the values $m=1,\,2\,,3$.

Next, we report a $\mathbb{P}_2$ solution for $m=4$ with a uniform mesh.

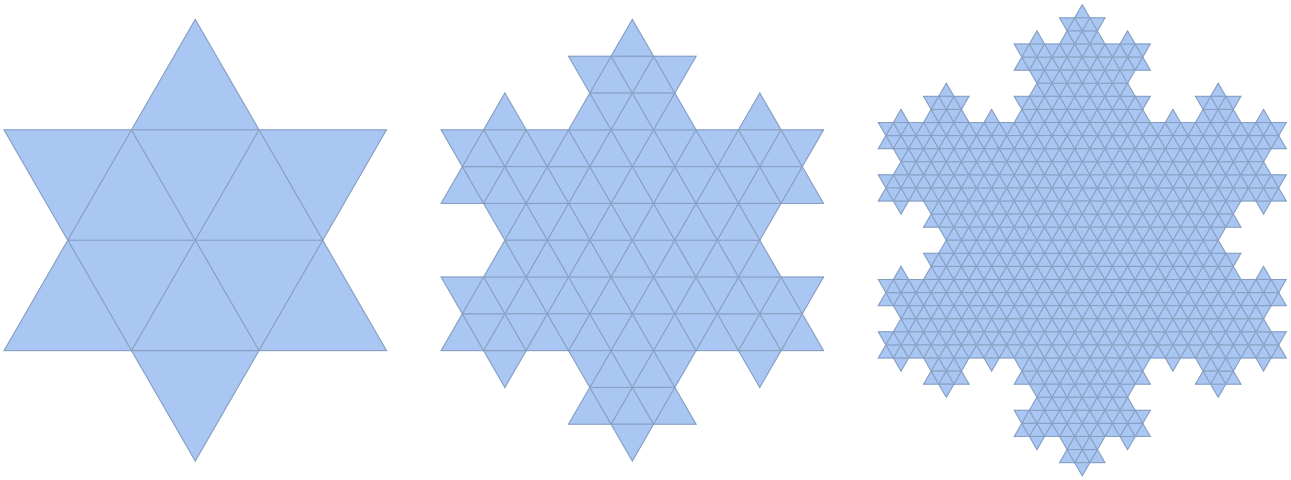

$m = 1.$ $m = 2.$ $m = 3.$

Figure 14 – The meshes, for $m = 1, 2, 3$.

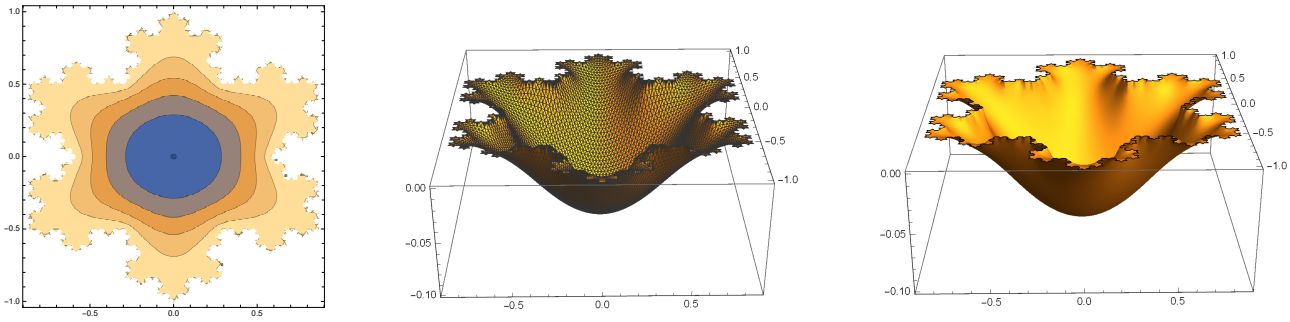

The contour plot of the solution. The meshed solution. The solution.

Figure 15 – The solution, in FEM_2^4, as a contour plot (left) and in 3D, meshed (center), or not (right).

5 Parametric Optimization

5.1 An Alternative Approach to the Membrane Problem

Given an (ϵ, δ)–domain (see Definition 2.5, on page 8), delimited by a d–set (for instance, the Koch Snowflake $\mathfrak{KS}$) and $f \in L^2(\mathring{\mathfrak{KS}})$, we are presently interested in the Poisson equation, in the case of Dirichlet boundary conditions; namely,

$$(\mathcal{P}_{\mathcal{H}}) \quad \left\{ \begin{array}{rcl} -\mathrm{div}\,(h\nabla u) & = f & \text{in } \mathring{\mathfrak{KS}}\,, \\ u & = 0 & \text{in } \partial\mathfrak{KS}\,, \end{array} \right.$$

where $h_{\min} \leqslant h \leqslant h_{\max}$. As is proved before, this equation admits a weak solution in the Sobolev space $W_2^1(\mathring{\mathfrak{KS}}) = H^1(\mathring{\mathfrak{KS}})$.

Since the bilinear form $a(.,.)$ is symmetric, we then deduce, thanks to the symmetric Lax–Milgram theorem ([Bre99], Corollary V.8, on page 84), that

$$u = \min_{v \in H_0^1(\mathring{\mathfrak{KS}})} \left\{ \Phi(v) = \frac{1}{2} \int_{\mathfrak{KS}} h\nabla v \nabla v \, dx - \int_{\mathfrak{KS}} f v \, dx \right\}. \tag{30}$$

By taking $e = \nabla v$, this is equivalent to

$$\min_{\substack{v\in H_0^1(\mathring{\mathfrak{KS}}),\, e\in L^2(\mathring{\mathfrak{KS}})^2\\ e=\nabla v}} \left\{ \Phi(v,e) = \frac{1}{2}\int_{\mathfrak{KS}} h\, e.e\, dx - \int_{\mathfrak{KS}} f v\, dx \right\}.$$

The intermediary Lagrangian of the problem is given by

$$\tilde{\mathcal{L}}(e,v,\lambda) = \Phi(v,e) + \int_{\mathfrak{KS}} \lambda.\left(\nabla v - e\right)\, dx\,.$$

The Lagrangian of the problem is then

$$\mathcal{L}(v,\lambda) = \min_{e\in L^2(\mathring{\mathfrak{KS}})} \tilde{\mathcal{L}}(e,v,\lambda)\,.$$

The map $e \mapsto \tilde{\mathcal{L}}(e,v,\lambda)$ is strongly convex and therefore admits a unique minimum given by the Euler equation $e^\star = h^{-1}\lambda$, which implies that

$$\begin{aligned}\mathcal{L}(v,\lambda) &= -\frac{1}{2}\int_{\mathfrak{KS}} h^{-1}\lambda.\lambda\, dx - \int_{\mathfrak{KS}} f v\, dx + \int_{\mathfrak{KS}} \lambda.\nabla v\, dx\\ &= -\frac{1}{2}\int_{\mathfrak{KS}} h^{-1}\lambda.\lambda\, dx - \int_{\mathfrak{KS}} v\left(\mathrm{div}(\lambda) + f\right)\, dx\,.\end{aligned}$$

The dual problem is then given by

$$\max_{\substack{\lambda\in L^2(\mathring{\mathfrak{KS}})^2\\ -\mathrm{div}(\lambda)=f}} \left\{ \Psi(\lambda) = \frac{1}{2}\int_{\mathfrak{KS}} h^{-1}\lambda.\lambda\, dx \right\}.$$

We thus obtain the following theorem:

Theorem 5.1 (**Existence of a Saddle Point Associated to the Lagrangian [All07]**). *There exists a unique saddle point (u,λ_u) associated to the Lagrangian $\mathcal{L}(v,\lambda)$ on $H_0^1(\mathring{\mathfrak{KS}}) \times L^2(\mathring{\mathfrak{KS}})^2$, given by*

$$\mathcal{L}(u,\lambda_u) = \max_{\lambda\in L^2(\mathring{\mathfrak{KS}})^2} \min_{v\in H_0^1(\mathring{\mathfrak{KS}})} \mathcal{L}(v,\lambda) = \min_{v\in H_0^1(\mathring{\mathfrak{KS}})} \max_{\lambda\in L^2(\mathring{\mathfrak{KS}})^2} \mathcal{L}(v,\lambda)\,,$$

with $\lambda_u = h\,\nabla u$.

5.2 Optimization Thickness of an Elastic Membrane on Fractals

In the following, we consider the problem of the optimal thickness h of a membrane deformed by a force f. We proceed as in [All07] in order to prove the existence of a solution. The thickness h is such that

$$\forall\, X \in \mathring{\mathfrak{KS}} : \quad 0 < h_{min} \leqslant h \leqslant h_{max}\,.$$

The behavior of the membrane is described by the Dirichlet problem

$$(\mathcal{P}_{\mathcal{H}}) \quad \left\{ \begin{array}{cc} -\mathrm{div}\left(h\nabla u\right) & = f \quad \text{in } \mathring{\mathfrak{KS}}\,,\\ u & = 0 \quad \text{in } \partial\mathfrak{KS}\,,\end{array}\right.$$

where $\mathring{\mathfrak{KS}}$ is the Koch Snowflake domain with fractal boundary $\partial\mathfrak{KS}$. The problem amounts in finding h in $\mathcal{H}$ which minimizes *the compliance* $J(h)$, given by

$$J(h) = \int_{\mathfrak{KS}} j(u_h)\, dx = \int_{\mathfrak{KS}} f\, u_h\, dx\,,$$

where

$$\mathcal{H} = \left\{ h \in L^\infty(\mathring{\mathfrak{KS}}) \text{ such that } 0 < h_{min} \leqslant h \leqslant h_{max} \text{ and } \int_{\mathfrak{KS}} h\, dx = h_0\, |\mathfrak{KS}| \right\},$$

and where u_h is the solution of the weak problem

$$\int_{\mathfrak{KS}} h \nabla u \nabla v\, dx = \int_{\mathfrak{KS}} f v\, dx\,.$$

The following lemmas establish the continuity of the operators $J : h \mapsto J(h)$ and $T : h \mapsto u_h$.

Lemma 5.2 (**[All07] proposition 5.1 p. 78**). *The functional $J : h \mapsto J(h)$ is continuous from $\mathcal{H}$ to $\mathbb{R}$.*

Lemma 5.3 (**[All07] lemma 5.3 p. 78**). *Let $h_n \in \mathcal{H}$ converging to $h^\star$ for the norm $L^\infty(\mathring{\mathfrak{KS}})$. Let u_{h_n} (resp. $u_{h^\star}$) the corresponding unique solution in $H_0^1(\mathring{\mathfrak{KS}})$ of the associated $(\mathcal{P}_\mathcal{H})$ problem. Then*

$$\lim_{n\to\infty} \|u_n - u\|_{H_0^1(\mathring{\mathfrak{KS}})} = 0 \tag{31}$$

In addition, by applying Theorem 5.1, on page 28, we deduce that

$$\int_{\mathfrak{KS}} f\, u_h dx = \min_{\substack{\lambda \in L^2(\mathring{\mathfrak{KS}})^2 \\ -\mathrm{div}(\lambda) = f}} \frac{1}{2} \int_{\mathfrak{KS}} h^{-1} |\lambda|^2\, dx\,.$$

The optimization problem then becomes

$$\inf_{h\in\mathcal{H}} \min_{\substack{\lambda \in L^2(\mathring{\mathfrak{KS}})^2 \\ -\mathrm{div}(\lambda) = f}} \frac{1}{2} \int_{\mathfrak{KS}} h^{-1}\, |\lambda|^2\, dx = \inf_{(h,\lambda)\in\mathcal{H}\times\mathcal{J}} \frac{1}{2} \int_{\mathfrak{KS}} h^{-1}\, |\lambda|^2\, dx\,, \tag{32}$$

where $\mathcal{J} = \left\{ \lambda \in L^2(\mathring{\mathfrak{KS}})^2, \quad -\mathrm{div}(\lambda) = f \quad \text{in } \mathring{\mathfrak{KS}} \right\}$. The set $\mathcal{H}\times\mathcal{J}$ is closed and convex as a product of two closed convex sets and the map $(h,\lambda) \mapsto \Psi(h,\lambda) = \dfrac{1}{2} \displaystyle\int_{\mathfrak{KS}} h^{-1} |\lambda|^2\, dx$ is convex, since the associated Hessian matrix is positive, continuous: Given $\lambda_n \in \mathcal{J}$ converging to $\lambda^\star$ for the norm $L^2(\mathring{\mathfrak{KS}})$, and $h_n \in \mathcal{H}$ converging to $h^\star$ for the norm $L^\infty(\mathring{\mathfrak{KS}})$, we have

$$\begin{aligned}
|\Psi(h,\lambda) - \Psi(h_n,\lambda_n)| &\leqslant \frac{1}{2} \int_{\mathfrak{KS}} |h^{-1}|\lambda|^2 - h_n^{-1}|\lambda_n|^2|\, dx \\
&\leqslant \frac{1}{2} \int_{\mathfrak{KS}} h^{-1} ||\lambda|^2 - |\lambda_n|^2| + |h^{-1} - h_n^{-1}||\lambda_n|^2\, dx \\
&\leqslant \frac{1}{2} \left(\frac{1}{h_{\min}} \|\lambda - \lambda_n\|_{L^2(\mathring{\mathfrak{KS}})} \|\lambda + \lambda_n\|_{L^2(\mathring{\mathfrak{KS}})} + \left\| \frac{h - h_n}{h\, h_n} \right\|_{L^\infty(\mathring{\mathfrak{KS}})} \|\lambda_n\|^2_{L^2(\mathring{\mathfrak{KS}})} \right) \\
&\leqslant \frac{1}{2} \left(\frac{1}{h_{\min}} \|\lambda - \lambda_n\|_{L^2(\mathring{\mathfrak{KS}})} \|\lambda + \lambda_n\|_{L^2(\mathring{\mathfrak{KS}})} + \frac{1}{h_{\min}^2} \|h - h_n\|_{L^\infty(\mathring{\mathfrak{KS}})} \|\lambda_n\|^2_{L^2(\mathring{\mathfrak{KS}})} \right) \\
&\to 0
\end{aligned}$$

and coercive, namely, for $(h_n, \lambda_n) \in \mathcal{H} \times \mathcal{J}$,

$$\lim_{\|(h_n,\lambda_n)\|\to+\infty} \Psi(h_n, \lambda_n) \geqslant \lim_{\|\lambda_n\|\to+\infty} \frac{\|\lambda_n\|^2_{L^2(\mathring{\mathfrak{KS}})}}{h_{\max}} = +\infty$$

The existence of the solution is ensured by the following theorem (see [CZ16] p. 125 for a more general version):

Theorem 5.4 (**[All07] theorem 3.8 and remark 3.9 p. 125**). *Let X be the dual space of a separable Banach space. Let $E \subset X$ be a non-empty convex closed subset. If $f : E \to \mathbb{R}$ is convex, continuous, and coercive, then f attains its minimum on E.*

We have the following result:

Theorem 5.5 (**[All07] lemma 5.25 p. 98**). *Given $\lambda \in L^2(\mathfrak{KS})^2$, the problem*

$$\min_{h\in\mathcal{H}} \frac{1}{2} \int_{\mathfrak{KS}} h^{-1}|\lambda|^2 \, dx$$

has a minimum $h(\lambda)$ in $\mathcal{H}$ given by

$$h(\lambda)(M) = \begin{cases} h^\star(M) = \dfrac{|\lambda(M)|}{\sqrt{l}} \text{ , if } h_{min} < h^\star < h_{max} \text{ ,} \\ h_{min} \text{ , if } h^\star \leqslant h_{min} \text{ ,} \\ h_{max} \text{ , if } h_{max} \leqslant h^\star \text{ ,} \end{cases}$$

where $l \in \mathbb{R}_+$ is the unique value such that $\displaystyle\int_{\mathfrak{KS}} h \, dx = h_0 \, |\mathfrak{KS}|$. This value is unique if $l > 0$.

5.3 Resolution by the Discrete Projected Gradient Algorithm (D.P.G.A.)

This section is based on the algorithm introduced by A. M. Toader in [Toa97] and described by G. Allaire in [All07]. Since the convergence of the finite element approximation has been proved, we can build a projected gradient algorithm on this approximation. We give next a convergence result for the $\mathbb{P}_1$ approximation. To this purpose, we set

$$\forall\, m \in \mathbb{N}^\star : \quad \mathbb{V}_{\delta_m} = \left\{ v \in C(\mathfrak{KS}_m); \quad v_{|\mathcal{T}_l^m} \in \mathbb{P}_1 \quad \forall\, \mathcal{T}_l^m \, in \, \mathcal{T}_{\delta_m}, \quad v_{|\partial\mathfrak{KS}_m} = 0 \right\} ;$$

$$\widetilde{\mathbb{V}}_{\delta_m} = \left\{ \tilde{v} \in C(\mathfrak{KS}); \quad \tilde{v}_{|\mathring{\mathfrak{KS}}_m} \in \mathbb{V}_{\delta_m}, \quad \tilde{v}_{|\mathring{\mathfrak{KS}}\setminus\mathring{\mathfrak{KS}}_m} = 0 \right\} .$$

$$\mathcal{H}_m = \left\{ h \in L^\infty(\mathring{\mathfrak{KS}}) : 0 < h_{min} \leqslant h \leqslant h_{max} \text{ on } \mathring{\mathfrak{KS}}_m, \quad h = 0 \text{ on } \mathring{\mathfrak{KS}} \setminus \mathring{\mathfrak{KS}}_m, \quad \int_{\mathfrak{KS}_m} h \, dx = h_0 \, |\mathfrak{KS}_m| \right\}$$

$$\mathcal{J}_m = \left\{ \lambda = h \, \nabla u, \quad (h,u) \in \mathcal{H}_m \times \widetilde{\mathbb{V}}_{\delta_m}, \quad -\mathrm{div}(h \, \nabla u) = f \quad \text{in } \mathring{\mathfrak{KS}}_m, \quad u = 0 \quad \text{in } \partial\mathfrak{KS}_m \right\} ,$$

and

$$\Psi(h, \lambda) = \frac{1}{2} \int_{\mathfrak{KS}} h^{-1} \, |\lambda|^2 \, dx \, .$$

We introduce the restriction operator, given by

$$\begin{aligned}\mathbf{R} \,:\, \mathcal{H} &\to \left\{ h \in L^\infty(\mathring{\mathfrak{KS}}) \,:\, 0 < h_{min} \leqslant h \leqslant h_{max} \text{ on } \mathring{\mathfrak{KS}}_m, \quad h = 0 \text{ on } \mathring{\mathfrak{KS}} \setminus \mathring{\mathfrak{KS}}_m \right\} \\ h &\to \mathbf{1}_{\mathring{\mathfrak{KS}}_m} h_{|\mathring{\mathfrak{KS}}_m}\,,\end{aligned}$$

along with the extension operator

$$\begin{aligned}\mathbf{E} \,:\, \mathcal{H}_m &\to \mathcal{H} \\ h &\to \tilde{h} \qquad \text{s.t.} \qquad \left(\tilde{h}\right)_{|\mathring{\mathfrak{KS}}_m} = h \qquad \text{and} \qquad \left(\tilde{h}\right)_{|\mathring{\mathfrak{KS}}\setminus\mathring{\mathfrak{KS}}_m} = \mathbf{P}_{\mathcal{H}}(h)\,,\end{aligned}$$

where $\mathbf{P}_{\mathcal{H}}(h) = \max\left(h_{\min}, \min(h_{\max}, h-l)\right)$ and where l is the solution of $\displaystyle\int_{\mathfrak{KS}} \mathbf{P}_{\mathcal{H}}(h)\,dx = h_0\,|\mathfrak{KS}|$.

We use the finite element discretization in order to introduce

$$\min_{(h,\lambda)\in\mathcal{H}_m\times\mathcal{J}_m} \Psi(h,\lambda)\,. \tag{33}$$

For any $m \in \mathbb{N}^\star$, the discrete projected gradient algorithm (D.P.G.A.) is given as follows:

Numerical algorithm:

1. Fix $h_0^m \in \mathcal{H}_m$.
2. For $n \geqslant 0$:
   (a) Compute $\lambda_n^m = h_n^m \nabla u_n^m$, where $u_n^m \in \widetilde{\mathbb{V}}_{\delta_m}$ is the unique solution of:

$$(\mathcal{P}_{\mathcal{H}_m}) \quad \left\{ \begin{array}{cc} -\mathrm{div}(h_n^m \nabla u_n^m) = f & \text{in } \mathring{\mathfrak{KS}}_m \\ u_n^m = 0 & \text{in } \partial\mathfrak{KS}_m \end{array} \right.$$

   (b) Update h:

$$h_{n+1}^m = \mathbf{P}_{\mathcal{H}_m}(h_n^m - \mu\,\partial_h\Psi(h_n^m, \lambda_n^m))$$

   where $\mu > 0$, $\mathbf{P}_{\mathcal{H}_m}(h) = \max(h_{\min}, \min(h_{\max}, h-l))$ and where l is the solution of

$$\int_{\mathfrak{KS}_m} \max(h_{\min}, \min(h_{\max}, h-l))\,dx = h_0\,|\mathfrak{KS}_m|\,.$$

   and we have that

$$\partial_h\Psi(h, \lambda_n^m) = -\frac{|\lambda_n^m|^2}{h^2}\,.$$

3. Stop when

$$|h_n^m - \mathbf{P}_{\mathcal{H}_m}(h_n^m - \mu\,\Psi'(h_n^m, \lambda_n^m))| < \varepsilon\,\mu\,h_{\max}\,.$$

The update can be written more explicitly

$$h_{n+1}^m = \mathbf{P}_{\mathcal{H}_m}\left(h_n^m + \mu\frac{|\lambda_n^m|^2}{(h_n^m)^2}\right). \tag{34}$$

The discrete projected gradient approximation is done in two steps:

$$h^\star \xrightarrow{\text{FEM}} h^{\star,m} \xrightarrow{\text{PGA}} h_{n^\star}^m$$

where we denote respectively by $h^\star$, $h^{\star,m}$ and $h_{n^\star}^m$, the respective solutions of the optimization problems (32), (33) and of equation (34). Let us introduce

$$\begin{array}{lcl} h^{\star,m} & \xrightarrow{\text{FEM}} & \lambda^{\star,m} \\ \tilde{h}^\star & \xrightarrow{\text{Continuous}} & \tilde{\lambda}^\star \\ \bar{h}^{\star,m} & \xrightarrow{\text{FEM}} & \bar{\lambda}^{\star,m} \\ h^\star & \xrightarrow{\text{Continuous}} & \lambda^\star \end{array}$$

where $h^{\star,m}$ and $h^\star$ stand respectively for the optimal thickness of discrete and continuous problems, $\tilde{h}^\star = \mathbf{E}(h^{\star,m})$ is the extension of $h^{\star,m}$ to $\mathring{\mathfrak{K}}\mathfrak{S}$ and $\bar{h}^{\star,m} = \mathbf{P}_{\mathcal{H}_m}(\mathbf{R}(h^\star))$ is the projected restriction of $h^\star$ on $\mathcal{H}_m$, we can check that

$$\begin{aligned} \|\bar{h}^{\star,m} - h^\star|_{L^\infty(\mathring{\mathfrak{K}}\mathfrak{S})} &\leqslant \|\bar{h}^{\star,m} - \mathbf{P}_{\mathcal{H}_m}(h^\star)\|_{L^\infty(\mathring{\mathfrak{K}}\mathfrak{S})} + \|\mathbf{P}_{\mathcal{H}_m}(h^\star) - h^\star\|_{L^\infty(\mathring{\mathfrak{K}}\mathfrak{S})} \\ &\leqslant \|\mathbf{R}(h^\star) - h^\star\|_{L^\infty(\mathring{\mathfrak{K}}\mathfrak{S})} + \|\mathbf{P}_{\mathcal{H}_m}(h^\star) - h^\star\|_{L^\infty(\mathring{\mathfrak{K}}\mathfrak{S})} \\ &\to 0 \end{aligned}$$

since $h^\star = \mathbf{P}_{\mathcal{H}}(h^\star)$ and

$$\lim_{m\to\infty}\left\|h^{\star,m} - \tilde{h}^\star\right\|_{L^\infty(\mathring{\mathfrak{K}}\mathfrak{S})} = \left\|\tilde{h}^\star\right\|_{L^\infty(\mathring{\mathfrak{K}}\mathfrak{S}\setminus\mathring{\mathfrak{K}}\mathfrak{S}_m)} = 0\,.$$

We therefore obtain the $L^\infty(\mathring{\mathfrak{K}}\mathfrak{S})$ convergence. Now, given the continuity of the solution operator $h \to u_h$ and the functional Ψ, for any real number $\varepsilon > 0$, we have that

$$-\varepsilon < \Psi(h^{\star,m},\lambda^{\star,m}) - \Psi(\tilde{h}^\star,\tilde{\lambda}^\star) \leqslant \Psi(h^{\star,m},\lambda^{\star,m}) - \Psi(h^\star,\lambda^\star) \leqslant \Psi(\bar{h}^{\star,m},\bar{\lambda}^{\star,m}) - \Psi(h^\star,\lambda^\star) < \varepsilon\,,$$

since

$$\Psi(h^\star,\lambda^\star) \leqslant \Psi(\tilde{h}^\star,\tilde{\lambda}^\star) \quad \text{and} \quad \Psi(h^{\star,m},\lambda^{\star,m}) \leqslant \Psi(\bar{h}^{\star,m},\bar{\lambda}^{\star,m})\,.$$

We also have convergence of the projected gradient algorithm on the prefractal domain:

Proposition 5.6 (**[Toa97]**). *Given $m \in \mathbb{N}$ and the prefractal domain $\mathfrak{KS}_m$, the projected gradient algorithm converges to the optimal solution $h^{\star,m}$.*

We have proved that:

Corollary 5.7.
The discrete projected gradient algorithm introduced in Section 5.3 converges to the optimal solution $h^\star$.

Proof. This directly follows from the triangle inequality; namely,

$$\|\Psi(h^\star,\lambda^\star)-\Psi(h^m_{n^\star},\lambda^m_{n^\star})\| \leqslant \|\Psi(h^\star,\lambda^\star)-\Psi(h^{\star,m},\lambda^{\star,m})\| + \|\Psi(h^{\star,m},\lambda^{\star,m})-\Psi(h^m_{n^\star},\lambda^m_{n^\star})\| \,,$$

where $n^\star$ denotes the optimal stopping iteration.

□

5.4 Numerical Results

In this last section, we represent the optimal solution of the compliance problem for the Koch Snowflake domain $\mathfrak{KS}$:

$$\min_{h\in\mathcal{H}} J(h) = \int_{\mathfrak{KS}} f\, u_h \, dx \,,$$

where

$$\mathcal{H} = \left\{ h \in L^\infty(\mathring{\mathfrak{KS}}) \text{ such that } 0.1 \leqslant h \leqslant 1 \text{ and } \int_{\mathfrak{KS}} h\, dx = \frac{1}{2}|\mathfrak{KS}| \right\}$$

and where u is the solution of

$$\begin{aligned} -\mathrm{div}\,(h\nabla u) &= e^{-(x^2+y^2)} && \text{in } \mathring{\mathfrak{KS}} \\ u &= 0 && \text{in } \partial\mathfrak{KS}\,. \end{aligned}$$

The approximation parameters are $m=4$, $\varepsilon=0.05$ and $\mu=0.05$.

The optimal thickness h in figure 17 presents oscillations up to the boundary, while the solution in figure 18 is smooth.

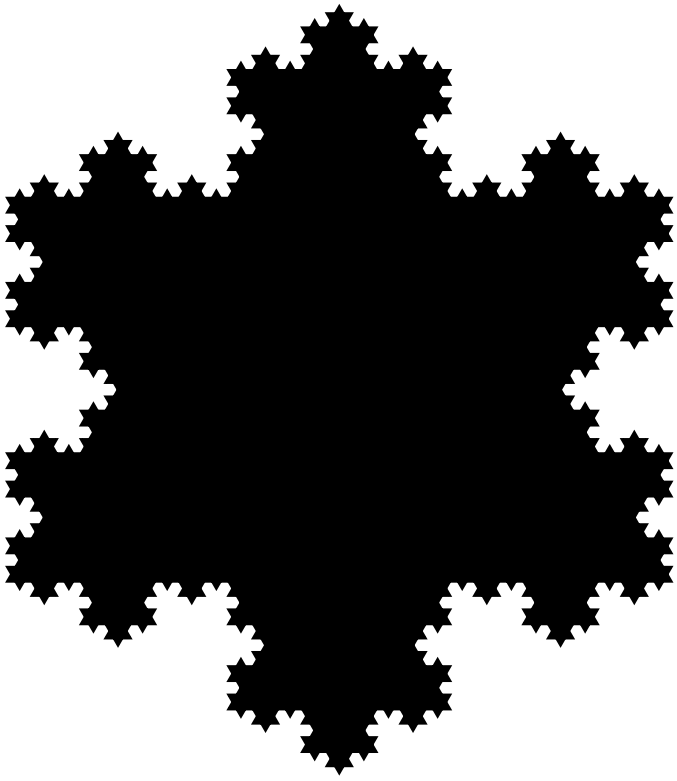

Figure 16 – The approximated domain $\mathfrak{KS}_4$.

Figure 17 gives a thrilling idea of the optimal shape:

1. The thickness does not vary radially from the center to the boundary, and it is not uniform near the boundary.
2. There are extreme thickness differences between neighboring regions near the boundary.
3. One can expect a self-similar structure of the shape as m approaches infinity.

The final form of the drum could be explained by the deformation properties of the snowflake membrane as explained By M. Lapidus and M. Pand in [LP95]. Approaching the boundary, the authors proved that the magnitude of the gradient of the ground state eigenfunction approaches 0 near acute angles of the approximation domain, while it tends to infinity near obtuse angles. This is exactly what is shown in figure 17: since the thickness is a positive function of the deformation, one can try to give the value $+1$ to obtuse angles and -1 to acute ones, by summing over a sub-region of the boundary, one can predict the color (mean thickness).

Upon zooming into the picture, we observe that the thickness value is not minimal at the center ($h = 0.125$). The minimal value is attained in specific regions near the corners, confirming the dumping phenomena near coastlines [LP95]. In the limit, we expect to observe a self-similar structure forming the minimal thickness regions in the image shown in Figure 22.

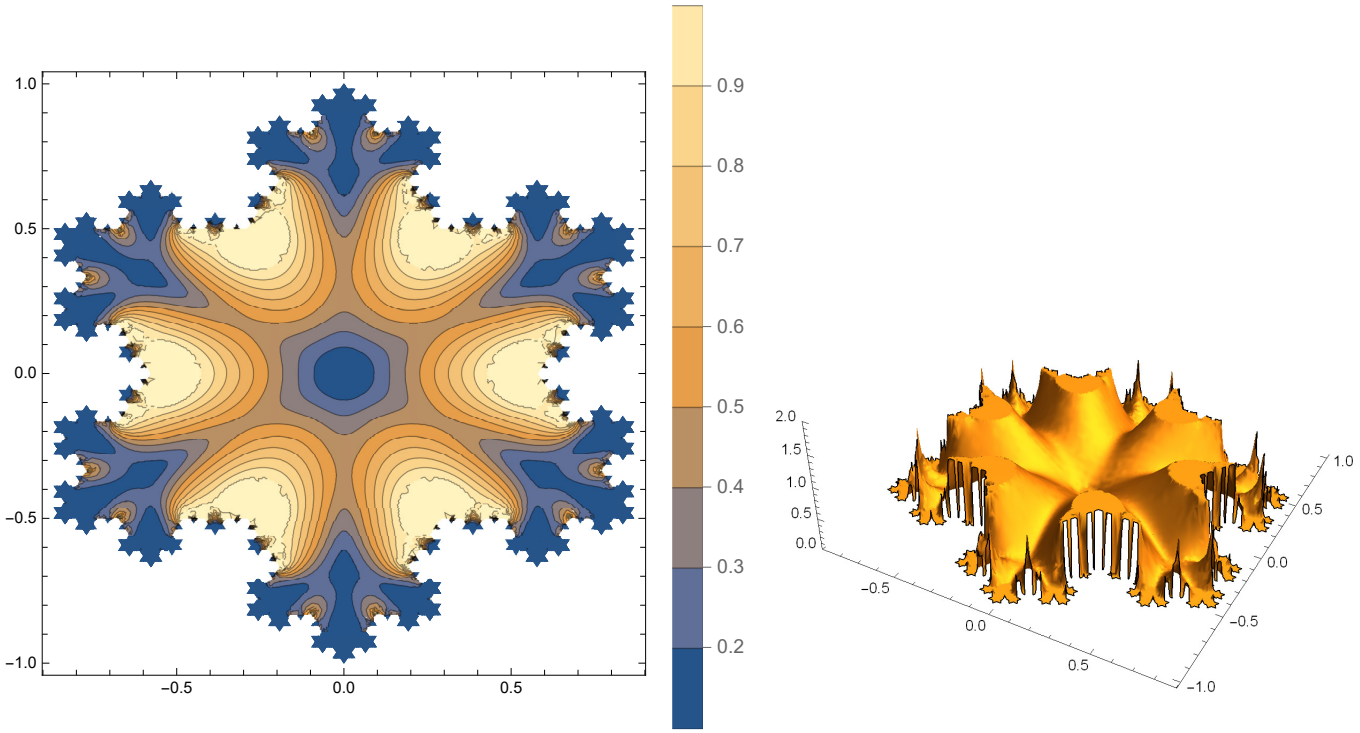

Figure 17 – Contour plot and 3D representation of the optimal thickness.

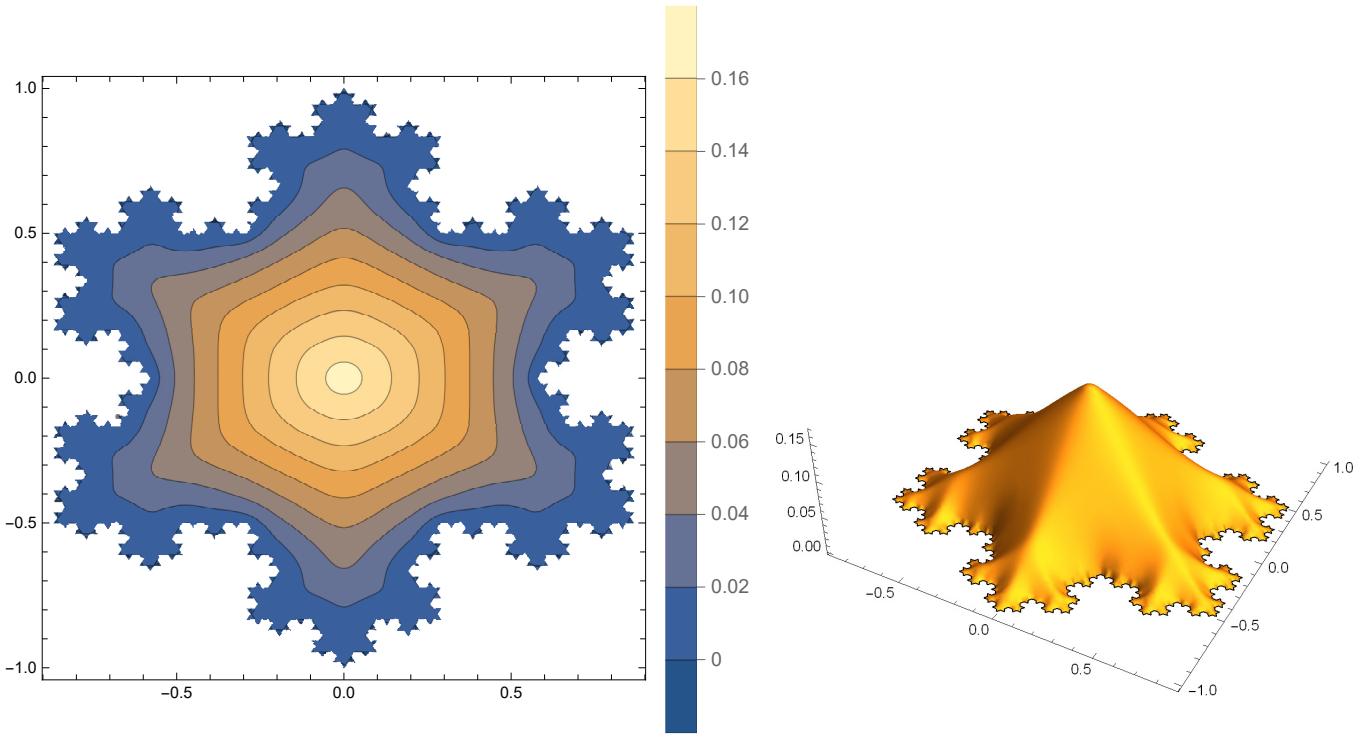

Figure 18 – Contour plot and 3D representation of the optimal solution.

6 Concluding Comments

The results of this work go far beyond the plain shape optimization of the Koch snowflake. In our mathematician's perspective, the Koch snowflake simply plays the role of a *model fractal membrane*. We intend to apply our results to fractal membranes which already exist in nature, more specifically, the plasma membrane of the Amoebozoa *Physarum polycephalum*, which presents an irregular appearance with numerous invaginations at multiple scales; see [Sau82]. This membrane is a dynamic structure, constantly changing as the organism moves, feeds, and explores its environment, which can display complex, adaptive behavior that can fold and unfold at various length scales, thus also exhibing a fractal-like organization. This dynamics is associated with oscillations.

This is not all. We believe that the oscillations associated with fractal-shaped membranes can be modelled – and understood – by applying the theory of Complex Dimensions, laid out for many years by Michel L. Lapidus and his collaborators; see [Lap91], [Lap92], [Lap93], [LP93], [LM95], [LvF00], [LP06], [Lap08], [LPW11], [ELMR15], [LvF13], [LRŽ17], [LRŽ18], [Lap19], [HL21] and [Lap24], in particular. The theory of Complex Dimensions is a very natural and intuitive way to characterize *fractality*, in connection with the intrinsic oscillations associated with fractals. The Complex Dimensions are obtained as the poles of fractal zeta functions, which can be viewed as (global) differential operators. Recent developments of the theory in [DL24b], [DL24a], [DL25], have shed new light on the connections between the Complex Dimensions and the eigenmodes of the fractal Laplacian issued from fractal cohomology; in particular, it is shown that a suitable truncation of the (infinite order) differential operator induced by the fractal zeta function enables us to obtain the fractal counterparts of classical operators, such as the Laplacian. We intend to go further, and numerically implement those results.

References

[All07] Grégoire Allaire. *Conception optimale de structures*. Springer, 2007.

[All12] Grégoire Allaire. *Analyse numérique et optimisation*. Éditions de l'École Polytechnique, Palaiseau, 2012.

[Bou04] Nicolas Bourbaki. *Theory of Sets*. Elements of Mathematics (Berlin). Springer-Verlag, Berlin, 2004. Reprint of the 1968 English translation [Hermann, Paris; MR0237342].

[Bre99] Haïm Brezis. *Analyse fonctionnelle : théorie et applications*. Dunod, Paris, 1999.

[CDMP19] María Eugenia Cejas, Irene Drelichman, and Javier C. Martínez-Perales. Improved fractional Poincaré type inequalities on John domains. *Arkiv för Matematik*, 57(2):285 – 315, 2019.

[Cia02] P. G. Ciarlet. *The Finite Element Method for Elliptic Problems*, volume 40 of *Classics in Applied Mathematics*. Society for Industrial and Applied Mathematics (SIAM), Philadelphia, PA, 2002.

[CRW13] Seng-Ke Chua, Scott Rodney, and Richard L. Wheeden. A compact embedding theorem for generalized Sobolev spaces. *Pacific journal of mathematics*, 265, 2013.

[CZ16] Kung Ching Chang and Tan Zhang. *Lecture Notes on Calculus of Variations*, volume 6. World Scientific, 2016.

[DL22] Claire David and Michel L. Lapidus. Weierstrass fractal drums - I - A glimpse of complex dimensions, 2022. URL: `https://hal.sorbonne-universite.fr/hal-03642326`.

[DL24a] Claire David and Michel L. Lapidus. From Weierstrass to Riemann: The Frobenius pass – When fractal flows come into play with zeta functions. In John Friedlander, Carl Pomerance, and Michael Th. Rassias, editors, *Essays in Analytic Number Theory – in Honor of Helmut Maier's 70^{th} Birthday*. Springer Nature, Cham, in press, 2024. URL: `https://hal.sorbonne-universite.fr/hal-04614665`.

[DL24b] Claire David and Michel L. Lapidus. Weierstrass fractal drums - II - Towards a fractal cohomology. *Mathematische Zeitschrift,* in press, 2024. URL: `https://hal.science/hal-03758820`.

[DL25] Claire David and Michel L. Lapidus. Revisiting microlocal analysis: A bridge between fractal cohomology and classical function spaces, 2025.

[ELMR15] Kate E. Ellis, Michel L. Lapidus, Michael C. Mackenzie, and John A. Rock. Partition zeta functions, multifractal spectra, and tapestries of complex dimensions. In M. Frame and N. Cohen, editors, *Benoît Mandelbrot: A Life in Many Dimensions*. The Mandelbrot Memorial, pages 267–322. World Scientific Publishers, Singapore and London, 2015. URL: `https://arxiv.org/abs/1007.1467`.

[Eva10] Lawrence C. Evans. *Partial differential equations*. American Mathematical Society, 2010.

[Fal03] Kenneth Falconer. *Fractal Geometry: Mathematical Foundations and Application.* Second Edition. John Wiley & Sons, Ltd, 2003.

[HL21] Hafedh Herichi and Michel L. Lapidus. *Quantized Number Theory, Fractal Strings and the Riemann Hypothesis: From Spectral Operators to Phase Transitions and Universality*. World Scientific Publishing, Singapore and London, 2021.

[HOP92] Dietmar Saupe Heinz-Otto Peitgen, Hartmut Jürgens. *Fractals for the Classroom. Part One: Introduction to Fractals and Chaos*. Number 1. Springer New York, NY, 1992.

[HS98] Olivier Haeberlé and Bernard Sapoval. Observation of vibrational modes of irregular drums. *Applied Physic Letters*, 73:33–57, 1998.

[Hut81] John E. Hutchinson. Fractals and self similarity. *Indiana University Mathematics Journal*, 30:713–747, 1981.

[Joh61] Fritz John. Rotation and strain. *Communications on pure and applied mathematics*, 14:391–413, 1961.

[Jon81] Peter Wilcox Jones. Quasiconformal mappings and extendability of functions in Sobolev spaces. *Acta Mathematica*, 147:71–88, 1981.

[JW84] Alf Jonsson and Hans Wallin. *Function Spaces on Subsets of* $\mathbb{R}^n$. Mathematical Reports (Chur, Switzerland). Harwood Academic Publishers, London, 1984.

[JW97] Alf Jonsson and Hans Wallin. Boundary value problems and brownian motion on fractals. *Chaos, Solitons & Fractals*, 8(2):191–205, 1997. Applications of Fractals in Material Science and Engineering.

[Lan02] Maria Rosaria Lancia. A transmission problem with a fractal interface. *Zeitschrift Für Analysis Und Ihre Anwendungen*, 21:113–133, 2002.

[Lap91] M. L. Lapidus. Fractal drum, inverse spectral problems for elliptic operators and a partial resolution of the Weyl-Berry conjecture. *Transactions of the American Mathematical Society*, 325:465–529, 1991.

[Lap92] M. L. Lapidus. Spectral and fractal geometry: From the Weyl-Berry conjecture for the vibrations of fractal drums to the Riemann zeta-function. In *Differential Equations and Mathematical Physics (Birmingham, AL, 1990)*, volume 186 of *Math. Sci. Engrg.*, pages 151–181. Academic Press, Boston, MA, 1992. URL: https://doi-org.accesdistant.sorbonne-universite.fr/10.1016/S0076-5392(08)63379-2.

[Lap93] M. L. Lapidus. Vibrations of fractal drums, the Riemann hypothesis, waves in fractal media and the Weyl-Berry conjecture. In *Ordinary and Partial Differential Equations, Vol. IV (Dundee, 1992)*, volume 289 of *Pitman Research Notes Mathematical Series*, pages 126–209. Longman Sci. Tech., Harlow, 1993.

[Lap08] Michel L. Lapidus. *In Search of the Riemann Zeros: Strings, Fractal Membranes and Noncommutative Spacetimes*. American Mathematical Society, Providence, RI, 2008.

[Lap19] Michel L. Lapidus. An overview of complex fractal dimensions: From fractal strings to fractal drums, and back. In *Horizons of Fractal Geometry and Complex Dimensions* (R. G. Niemeyer, E. P. J. Pearse, J. A. Rock and T. Samuel, eds.), volume 731 of *Contemporary Mathematics*, pages 143–265. American Mathematical Society, Providence, RI, 2019. URL: https://arxiv.org/abs/1803.10399.

[Lap24] Michel L. Lapidus. *From Complex Fractal Dimensions and Quantized Number Theory To Fractal Cohomology: A Tale of Oscillations, Unreality and Fractality, to appear*. World Scientific Publishing, Singapore and London, 2024.

[LM95] M. L. Lapidus and H. Maier. The Riemann hypothesis and inverse spectral problems for fractal strings. *Journal of the London Mathematical Society. Second Series*, 52(1):15–34, 1995. URL: https://doi-org.accesdistant.sorbonne-universite.fr/10.1112/jlms/52.1.15.

[LNRG96] Michel L. Lapidus, John W. Neuberger, Robert J. Renka, and Cheryl A. Griffith. Snowflake harmonics and computer graphics: Numerical computation of spectra on fractal drums. *International Journal of Bifurcation and Chaos*, pages 1185–1210, 1996.

[LP93] M. L. Lapidus and C. Pomerance. The Riemann zeta-function and the one-dimensional Weyl-Berry conjecture for fractal drums. *Proceedings of the London Mathematical Society. Third Series*, 66(1):41–69, 1993. URL: https://doi-org.accesdistant.sorbonne-universite.fr/10.1112/plms/s3-66.1.41.

[LP95] Michel L. Lapidus and Michael M. H. Pang. Eigenfunctions of the Koch snowflake domain. *Communications in Mathematical Physics*, 172(2):359 – 376, 1995.

[LP06] Michel L. Lapidus and Erin P. J. Pearse. A tube formula for the Koch snowflake curve, with applications to complex dimensions. *Journal of the London Mathematical Society. Second Series*, 74(2):397–414, 2006. URL: https://doi-org.accesdistant.sorbonne-universite.fr/10.1112/S0024610706022988.

[LPW11] M. L. Lapidus, E. P. J. Pearse, and S. Winter. Pointwise tube formulas for fractal sprays and self-similar tilings with arbitrary generators. *Advances in Mathematics*, 227(4):1349–1398, 2011. URL: https://doi-org.accesdistant.sorbonne-universite.fr/10.1016/j.aim.2011.03.004.

[LRŽ17] Michel L. Lapidus, Goran Radunović, and Darko Žubrinić. Distance and tube zeta functions of fractals and arbitrary compact sets. *Advances in Mathematics*, 307:1215–1267, 2017.

[LRŽ18] Michel L. Lapidus, Goran Radunović, and Darko Žubrinić. Fractal tube formulas for compact sets and relative fractal drums: Oscillations, complex dimensions and fractality. *Journal of Fractal Geometry*, 5(1):1–119, 2018.

[Luc04] Brigitte Lucquin. *Equations aux dérivées partielles et leurs approximations*. Ellipses, 2004.

[LvF00] Michel L. Lapidus and Machiel van Frankenhuijsen. *Fractal Geometry and Number Theory: Complex Dimensions of Fractal Strings and Zeros of Zeta Functions*. Birkhäuser Boston, Inc., Boston, MA, 2000.

[LvF13] Michel L. Lapidus and Machiel van Frankenhuijsen. *Fractal Geometry, Complex Dimensions and Zeta Functions: Geometry and Spectra of Fractal Strings*. Springer Monographs in Mathematics. Springer, New York, second revised and enlarged edition (of the 2006 edition), 2013.

[Man83] Benoît B. Mandelbrot. *The Fractal Geometry of Nature*. English translation, revised and enlarged edition (of the 1977 edition). W. H. Freeman & Co, New York, 1983.

[Mar48] Andreï A. Markov. *Selected Works (in Russian*. Moscow-Leningrad, 1948.

[Nys94] Kaj Nyström. *Smoothness Properties of Solutions to Dirichlet Problems in Domains with a Fractal Boundary*. PhD thesis, 1994. URL: `https://urn.kb.se/resolve?urn=urn:nbn:se:umu:diva-8445`.

[Nys96] Kaj Nyström. Integrability of Green potentials in fractal domains. *Arkiv för Matematik*, 34(2):335 – 381, 1996.

[Pom92] Christian Pommerenke. *Boundary Behaviour of Conformal Maps*. Number 1. Springer Berlin, Heidelberg, 1992.

[RJM04] Pierre-Arnaud Raviart and Jean-MarieThomas. *Introduction à l'analyse numérique des équations aux dérivées partielles*. Dunod, Paris, 2004.

[Sap89] Bernard Sapoval. Experimental observation of local modes in fractal drums. *Physica D*, 38:296–298, 1989.

[Sau82] Helmut W. Sauer. *Developmental biology of Physarum*. Developmental and cell biology series 11. Cambridge University Press, Cambridge, 1982.

[SG93] Bernard Sapoval and Thierry Gobron. Vibrations of strongly irregular or fractal resonators. *Physical Review E*, 47:3013–3024, May 1993. URL: `https://link.aps.org/doi/10.1103/PhysRevE.47.3013`.

[SGM91] Bernard Sapoval, Thierry Gobron, and A. Margolina. Vibrations of fractal drums. *Physical Review Letters*, 67:2974–2977, Nov 1991.

[Toa97] A. M. Toader. Convergence of an algorithm in optimal design. *Structural Optimization*, 13:195–198, 1997.

[Wal91] Hans Wallin. The trace to the boundary of Sobolev spaces on a snowflake. *Manuscripta Mathematica*, 73:117–125, 1991.

[Wal92] Hans Wallin. Self–similarity, Markov's Inequality and d–sets. In *Constructive Theory of Functions, Varna '91*, pages 285–297, 1992.

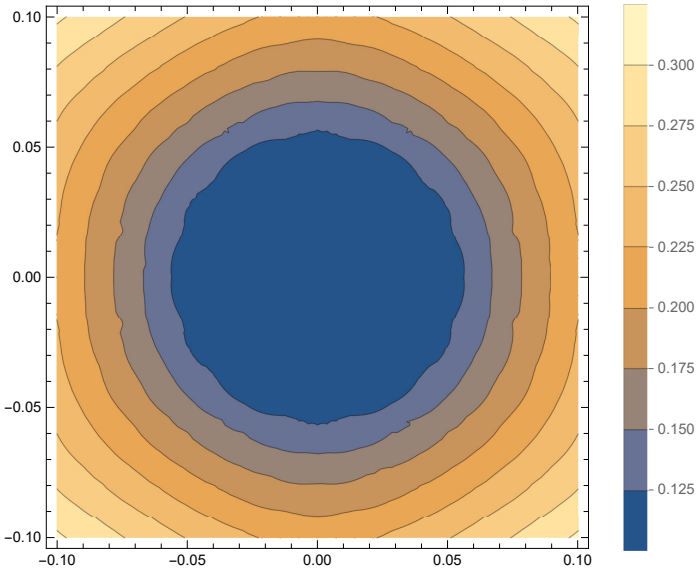

Figure 19 – The center of the snowflake.

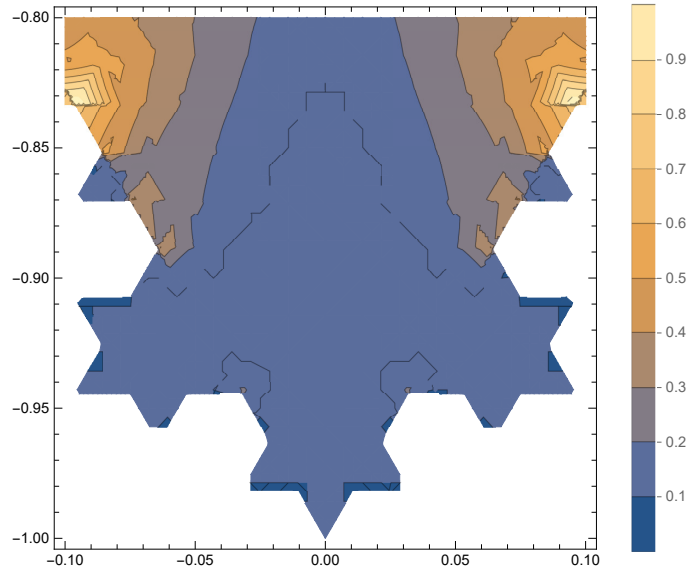

Figure 20 – The south corner.

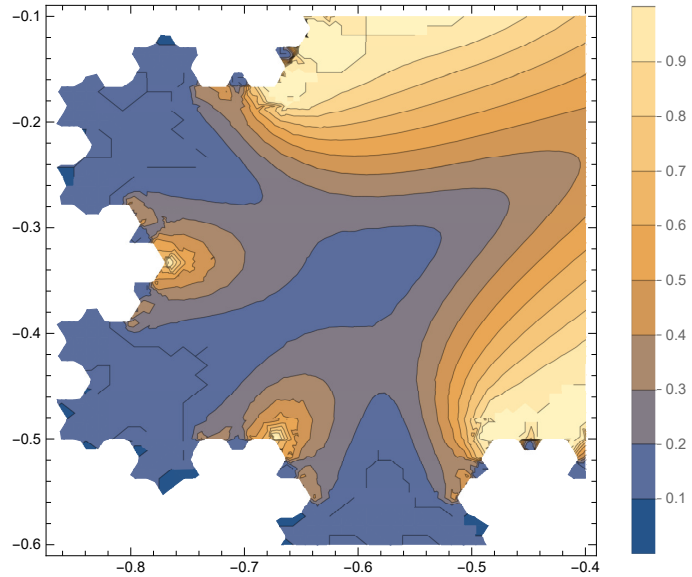

Figure 21 – The south west corner.

Figure 22 – Zoom on the thickness.